AD_____

Award Number: DAMD17-98-1-8224

TITLE: Applications of a Novel Nucleic Acid Detection Method in
Breast Cancer Analysis of Overexpression of HER-2/neu and FAK

PRINCIPAL INVESTIGATOR: Herbert Thorp, Ph.D.

CONTRACTING ORGANIZATION: University of North Carolina
                            Chapel Hill, North Carolina 27599-1350

REPORT DATE: July 2001

TYPE OF REPORT: Annual

PREPARED FOR: U.S. Army Medical Research and Materiel Command
                Fort Detrick, Maryland 21702-5012

DISTRIBUTION STATEMENT: Approved for Public Release;
                        Distribution Unlimited

The views, opinions and/or findings contained in this report are
those of the author(s) and should not be construed as an official
Department of the Army position, policy or decision unless so
designated by other documentation.

20020814 206

REPORT DOCUMENTATION PAGE

Public reporting burden for this collection of information is estimated to average 1 hour per response, including the time for reviewing instructions, searching existing data sources, gathering and maintaining the data needed, and completing and reviewing this collection of information. Send comments regarding this burden estimate or any other aspect of this collection of information, including suggestions for reducing this burden to Washington Headquarters Services, Directorate for Information Operations and Reports, 1215 Jefferson Davis Highway, Suite 1204, Arlington, VA 22202-4302, and to the Office of Management and Budget, Paperwork Reduction Project (0704-0188), Washington, DC 20503

1. AGENCY USE ONLY (Leave blank)	2. REPORT DATE July 2001	3. REPORT TYPE AND DATES COVERED Annual (1 Jul 00 – 30 Jun 01)

4. TITLE AND SUBTITLE
Applications of a Novel Nucleic Acid Detection Method in Breast Cancer Analysis of Overexpression of HER-2/neu and FAK

5. FUNDING NUMBERS
DAMD17-98-1-8224

6. AUTHOR(S)
Herbert Thorp, Ph.D.

7. PERFORMING ORGANIZATION NAME(S) AND ADDRESS(ES)
University of North Carolina
Chapel Hill, North Carolina 27599-1350

E-Mail: holden@unc.edu

8. PERFORMING ORGANIZATION REPORT NUMBER

9. SPONSORING / MONITORING AGENCY NAME(S) AND ADDRESS(ES)

U.S. Army Medical Research and Materiel Command
Fort Detrick, Maryland 21702-5012

10. SPONSORING / MONITORING AGENCY REPORT NUMBER

11. SUPPLEMENTARY NOTES

12a. DISTRIBUTION / AVAILABILITY STATEMENT
Approved for Public Release; Distribution Unlimited

12b. DISTRIBUTION CODE

13. ABSTRACT (Maximum 200 Words)

The proposal "Applications of a Novel Nucleic Acid Detection Method in Breast Cancer: Analysis of Overexpression of HER-2/neu and FAK" is aimed at utilizing new biosensors based on guanine electron transfer to quantitate messenger RNA for breast cancer genes. The biosensors are based on a scheme involving abstraction of electrons from the guanines of immobilized RNA to generate a signature current for a specific gene. The purpose of the proposed research is to demonstrate that the guanine electron transfer technology can be used to detect overexpressed RNAs in real biological samples. In the first year, electrochemical detection of specific genes using $Ru(bpy)_3^{2+}$-mediated electrochemistry was demonstrated. In the second year, fragment size was determined using electrochemistry, which may enable new methods for RFLP analysis or detecting microsatellites. This year, novel molten salts of DNA were prepared that can be immobilized on small electrodes for ultra-miniaturized detection. These materials have allowed for electrochemical detection of DNA on microlocations as small as 5 microns; present DNA chips are generally limited to microlocations in the 100 micron range.

14. SUBJECT TERMS
breast cancer, automated nucleic acid detection, gene expression, mRNA quantitation, prognostic markers, protein kinases

15. NUMBER OF PAGES
30

16. PRICE CODE

17. SECURITY CLASSIFICATION OF REPORT	18. SECURITY CLASSIFICATION OF THIS PAGE	19. SECURITY CLASSIFICATION OF ABSTRACT	20. LIMITATION OF ABSTRACT
Unclassified	Unclassified	Unclassified	Unlimited

Table of Contents

Introduction

The project "Applications of a Novel Nucleic Acid Detection Method in Breast Cancer: Analysis of Overexpression of HER-2/neu and FAK" is aimed at utilizing new biosensors based on guanine electron transfer to quantitate messenger RNA for breast cancer genes. The biosensors are based on a scheme involving abstraction of electrons from the guanines of immobilized RNA to generate a signature current for a specific gene. The purpose of the proposed research is to demonstrate that the guanine electron transfer technology can be used to detect overexpressed RNAs in real biological samples. (Note that changes in the Statement of Work were approved during the last year as was a one-year, no-cost extension). The first Task involves demonstration of electrochemical detection of specific genes using $Ru(bpy)_3^{2+}$-mediated electrochemistry (bpy = 2,2'-bipyridine); this task was completed and described in the first report. The second task involves detection of fragment size using electrochemistry; this task was completed and described in the second report. The third task involves preparing liquid DNA samples that can be immobilized on small electrodes for ultra-miniaturized detection. The completion of this task is described in this report.

Body

The studies on Task 1 have now been published. The first paper, "Modification of Metal Oxides with Nucleic Acids: Detection of Attomole Quantities of Immobilized DNA by Electrocatalysis," was in press when the last report was filed but has since been printed.[1] More detailed studies on the kinetics of electron transfer at these interfaces have since been published as "Oxidation Kinetics of Guanine in DNA Molecules Adsorbed to Indium Tin Oxide Electrodes," which is now attached to this report.[2]

The studies on Task 2 have now been published. The proof-of-principle on the concept that longer fragments containing guanine give larger signals was demonstrated in solution and published as "Kinetics of Metal-Mediated, One-Electron Oxidation of Guanine in Polymeric DNA and Oligonucleotides Containing Trinucleotide Repeat Sequences," which is attached.[3] A second paper demonstrating this concept on electrode surfaces has been submitted to Analytical Chemistry and is undergoing second review following acceptance with revisions. A copy will be attached to the final report after this paper is printed. These studies were described in the last annual report.

The studies for Task 3 have been completed. These experiments center on forming molten salts of DNA that can be interrogated on very small (5 μm) electrodes. Studies on the formation and interrogation of these compounds have been published as "An Ionic Liquid Form of DNA: Redox-Active Molten Salts of Nucleic Acids," which is attached.[4] This work is now described.

We have prepared novel ionic liquid materials based on DNA salts of polyether-decorated transition metal complexes (Figure 1) that, in undiluted form, undergo electrochemical reactions and act as catalytic electron relays between a microelectrode and DNA. The DNA remains double-stranded in the ionic liquids, and the electrochemistry is performed under vacuum. The semi-solid state nature of the new DNA materials—which can be regarded as molten salts—may be useful in microelectronic circuits that utilize DNA for *both* self-assembly and electronic

connections. Further, the ability to control DNA sequence and secondary structure will allow creation of new classes of molten materials that undergo well defined structural changes programmed by sequence and monitored by electrochemical signals.
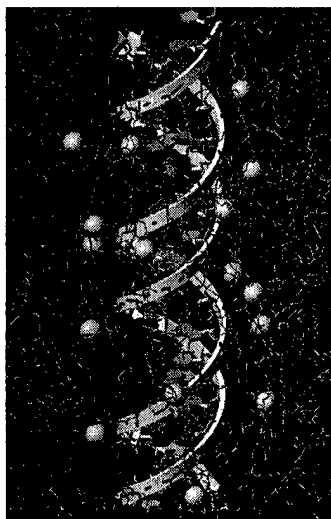

Figure 1. Pictorial representation of DNA melt with poly(ethylene oxide)-tailed metal complexes (silver balls) surrounding the nucleic acid. Chemical structures are given in Figure 2.

DNA redox chemistry. The Thorp group is well known for establishing that the one-electron oxidation of the guanine base can be realized at solid electrodes using conventional electrochemical techniques in conjunction with redox catalysts. This one-electron oxidation has been extensively scrutinized as a partial origin of oxidative DNA damage and as a probe of long-range electron transfer along the DNA helix. Transient formation of oxidized guanine bases appears to play a critical role in the ability of DNA to mediate remote electron transfer between two attached circuit elements where those circuit elements can either be molecular donors and acceptors or electrodes. Transition metal complexes with potentials ≥ 1.0 V, such as $Ru(bpy)_3^{2+}$ (bpy = 2,2'-bipyridine), mediate guanine electron transfer from intact DNA molecules according to the reaction scheme:[5]
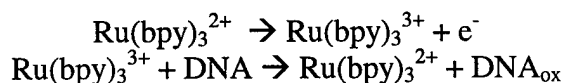
$$Ru(bpy)_3^{2+} \rightarrow Ru(bpy)_3^{3+} + e^-$$
$$Ru(bpy)_3^{3+} + DNA \rightarrow Ru(bpy)_3^{2+} + DNA_{ox}$$

where DNA_{ox} is a DNA molecule with a guanine residue that is oxidized by one electron. The electrochemical signal is a sensitive probe of the DNA structure; distinctly different signals are observed for guanines in single strands, duplexes, and G quartets. In addition, a variety of non-native nucleobases (such as 7-deazaguanine, 7-deazaadenine, 8-oxo-guanine, 5-aminocytosine, and 5-aminouridine) have been identified that have distinct redox potentials and provide unique signals at potentials lower than that of guanine.[6] These non-native nucleobases can be readily incorporated by common polymerases into

large DNA or RNA molecules that can be detected at lower potentials using appropriately matched redox catalysts.
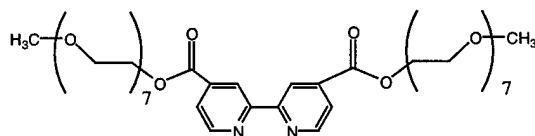
MePEG-bpy

1: Co(MePEG-bpy)$_3$(ClO$_4$)$_2$
2: Fe(MePEG-bpy)$_3$(ClO$_4$)$_2$
3: Co(MePEG-bpy)$_3$•DNA

Figure 2. Chemical structures of melt-forming cations.

In addition to the electrochemical signals, the guanine oxidation can also be detected on the nucleic acid side of the reaction using high-resolution gel electrophoresis with radiolabeled nucleic acids. In this experiment, the radiolabeled DNA is photolyzed in the presence of Ru(bpy)$_3^{2+}$ and a sacrificial electron acceptor, such as Fe(CN)$_6^{3-}$. The excited Ru(bpy)$_3^{2+}$ then transfers an electron to the acceptor, which generates Ru(bpy)$_3^{3+}$, which can abstract an electron from guanine. Base treatment of the DNA then leads to strand scission at the oxidized guanine, which can be visualized using high-resolution gel electrophoresis. The extent of strand scission at a particular guanine is directly related to the rate of electron transfer for that same residue, which allows correlation of the real-time electrochemistry and the electrophoresis experiment. This approach has been used to study the effects of secondary structure on the rates of guanine oxidation. In addition, stacking two guanines in a DNA sequence produces enhanced reactivity at the 5' guanine in duplex DNA. This effect is a sensitive probe of DNA structure that we have applied to single strands, duplexes, DNA-RNA hybrids, and G quartets.

Polyether Redox Melts. Room-temperature melts are reliably formed when one partner in a cation:anion pair is decorated with poly(ethylene glycol) tails of appropriate length (Figure 2) and are redox-active molten salts when one of the partners is also capable of electron transfer. This area of research has been pioneered over the last ten years by our collaborator, Professor Royce Murray. The polyether tail can be attached to either the redox-active partner or the redox-inert counterion. For example, the perchlorate salt Co(MePEG-bpy)$_3$(ClO$_4$)$_2$ (**1**), containing a redox-active metal complex with polyether tails, is a molten material. When this highly viscous, amorphous compound is placed on a three-electrode array containing a 3.9 μm radius Pt microelectrode, an electrochemical signal due to the Co(III/II) oxidation reaction (0.18 V, all potentials in the text are versus Ag/AgCl) is observed in the neat liquid. Diffusion-controlled currents in polyether melts reflect the summed rates of physical diffusion of the metal complex to the microelectrode and of electron hopping (self-exchange) between oxidized and reduced forms of the complex in the melt. For the Co(III/II) wave observed in **1**, electron hopping is slow, and the observed current is solely a function of physical diffusion. When Co is replaced with Fe to form Fe(MePEG-bpy)$_3$(ClO$_4$)$_2$ (**2**), the Fe(III/II) oxidation wave appears at 1.04 V and electron hopping is much faster (while physical diffusion remains constant), giving higher overall currents.

Faster electron hopping for Fe(III/II) compared to Co(III/II) is a chemically well understood difference.

DNA ionic liquid. A DNA melt was prepared by equilibrium dialysis of a solution of **1** and herring testes DNA at a stoichiometry of two nucleotides of DNA per one dicationic Co complex. After extensive dialysis to remove the perchlorate counterions from **1** and the sodium cations from DNA, the solution was placed on a rotary evaporator to yield a highly viscous melt, Co(MePEG-bpy)$_3$•DNA (**3**). The most surprising feature about the nucleic acid melts is that the *DNA remains double-stranded*, which was confirmed by gel electrophoresis and CD spectroscopy. A pictorial representation of **3** showing the relative sizes of the polyether tails and DNA is shown in Figure 1. Apparently, the polyether tails provide an environment where the biomolecule can maintain its native structure, suggesting that a number of biomolecular structures might be stabilized in the polyether environment.

The only electrochemical signal seen in melt **3** is that due to the Co(III/II) couple. Co(III) is not a sufficiently powerful oxidant to oxidize guanine. However, when a 1:1 mixture was made of **3** and the iron perchlorate melt **2**, two electrochemical signals were observed. The first was due to the Co(III/II) wave, while the more positive wave for Fe(III/II) displayed an oxidation current much larger than the subsequent reductive current; the electrochemical behavior of this wave was indicative of catalytic oxidation of guanine in DNA by the Fe(III). The melt was doped with a radiolabeled oligonucleotide, which was used to show that the Fe(III) complex oxidized guanine. We therefore ascribe the catalytic current observed to oxidation of guanine by Fe(III) *in the neat DNA molten salt*. Thus, this experiment shows that the catalytic oxidation pioneered by the Thorp group as a means for detection of DNA can be observed at electrodes as small as 5 μm.

Experimental. *Materials and measurements.* Compounds **1** and **2** were prepared according to a published procedure[7] and characterized by NMR and electrochemistry. The MePEG-NEt$_3$Cl salt was prepared according to a published procedure.[8] Electrochemical measurements were conducted under vacuum at 67°C on 3-electrode arrays with a 3.9 μm-radius Pt working electrode as previously described.[7] CD spectra were acquired on an Aviv Model 62DS Circular Dichroism Spectrometer with a 0.1 cm cell. Values of D_{PHYS} were determined from chronoamperometry data plotted as current versus $t^{-1/2}$; and linear fits were used to determine D_{PHYS} as described previously.[7] The bulk concentration of the Co complex was 0.4 M in **3** and 0.2 M in the 1:1 **3/2** melt.

Preparation of DNA ionic liquids. Herring testes DNA was obtained from Sigma and sheared to a size range of 50-100 bp as determined by agarose gel electrophoresis. To form compound **3**, 41.0 mL of 49 mM sheared HT DNA (2.0 mmol) were added to 1.0 mmol of **1**. The solution was diluted to 300 mL and added to Millipore brand 500 MWCO dialysis tubing that had been soaked twice for 30 min in nanopure water. Dialysis was executed for 1 week during which the 8-L reservoir was replaced every 12 h. Following dialysis, the solution was removed from the dialysis tubing, and the water was removed by rotary evaporation at ambient temperature. The resulting melt was rinsed repeatedly with nanopure water. Removal of water produces a viscous, transparent material that was further dried under vacuum. Elemental analysis gave P = 1.90%, Na = 0.04%, Cl = 0.77%, and Co = 1.90%. Complete conversion to Co(MePEG-bpy)$_3$•DNA

would give P = 1.75%, Na = 0%, Cl = 0%, and Co = 1.66%. Compound **4** was prepared by the same method except that 2 mmol of MePEG-NEt$_3$Cl was used as was 100 MWCO dialysis tubing. Elemental analysis of **4** gave P = 4.63%, Na = 0.20%, and Cl = 0.87%. Complete conversion to MePEG-NEt$_3$•DNA would give P = 3.90%, Na = 0%, and Cl = 0%.

Gel electrophoresis. Compound **2** was oxidized to the Fe(III) form by reaction with 1 equivalent of Ce(ClO$_4$)$_4$ + 2HClO$_4$ in an acetonitrile/perchloric acid solution (GFS Chemicals, Powell, OH). Complete oxidation to the Fe(III) form was confirmed by absorbance spectroscopy. In the cleavage reactions, a 10-μL solution of 5'-^{32}P labeled oligonucleotide (5'-AAAAATATAGTATAAAAAA-3') and one equivalent of calf thymus DNA was mixed with 10 μL of either a 1 mM solution of oxidized **2**, **2** that had not been oxidized, or Ce(IV) alone. The reaction was allowed to proceed until the Fe(III) was converted to Fe(II) (the color of the solution changed from green to violet). The samples were ethanol precipitated, piperidine treated, and electrophoresed on a denaturing polyacrylamide gel according to a published procedure.[9] A single cleavage site was detected on the gel at the guanine nucleotide upon reaction with oxidized **2** (the site of reaction was determined by comparison with a Maxam-Gilbert G reaction). No cleavage was observed upon reaction with **2** that had not been oxidized or with Ce(IV) in the absence of **2**.

Research Accomplishments

- Developed new molten salts of DNA based on polyether-tailed counterions.
- Characterized molten salts by elemental analysis and UV spectroscopy.
- Detected DNA electrochemically by catalytic guanine oxidation inside the molten salts.

Reportable Outcomes

- Immobilization method reported in Analytical Chemistry: Modification of Metal Oxides with Nucleic Acids: Detection of Attomole Quantities of Immobilized DNA by Electrocatalysis. P. M. Armistead, H. H. Thorp* *Anal. Chem.* **2000**, *72*, 3764-3770 (note this paper was listed and given in the last report but had not yet been printed).
- Kinetics studies of oxidation at the modified electrodes published in Analytical Chemistry (listed as submitted on the previous report): Oxidation Kinetics of Guanine in DNA Molecules Adsorbed to Indium Tin Oxide Electrodes. P. M. Armistead, H. H. Thorp* *Anal. Chem.* **2001**, *73*, 558-564. (Note that P. M. Armistead also received fellowship support from DoD as DAMD17-96-1-6067.)
- Kinetics of fragment size effects in solution reported in a paper submitted to Inorganic Chemistry (listed as submitted on the previous report): Kinetics of Metal-Mediated, One-Electron Oxidation of Guanine in Polymeric DNA and Oligonucleotides Containing Trinucleotide Repeat Sequences. I. V. Yang, H. H. Thorp* *Inorg. Chem.* **2000**, *39*, 4969-4976.

- Detection of fragment size on modified electrodes under second review at Analytical Chemistry: Modification of Indium Tin Oxide Electrodes with Repeat Polynucleotides: Electrochemical Detection of Trinucleotide Repeat Expansion. I. V. Yang, H. H. Thorp* *Anal. Chem.*, submitted.
- Synthesis of molten salts of DNA, characterization of these salts, and detection of DNA inside the molten salts published in Journal of the American Chemical Society: An Ionic Liquid Form of DNA: Redox-Active Molten Salts of Nucleic Acids. A. M. Leone, S. C. Weatherly, M. E. Williams, R. W. Murray*, H. H. Thorp* *J. Am. Chem. Soc.* **2001**, *123*, 218-222.

Conclusions

The work performed under this grant has provided a convenient method for immobilizing PCR fragments and quantitating these fragments quickly (Task 1). The method can also be used to determine the size of PCR fragments, which will allow for detection of genetic abnormalities, RFLP analysis, detection of trinucleotide repeat expansion, and monitoring other changes that are reflected in the size of DNA fragments (Task 2). In this report, preparation of novel materials comprising DNA molten salts is described.[4] This work constitutes the completion of Task 3. Studies aimed at completing Task 4 are now underway.

References

(1) Armistead, P. M.; Thorp, H. H. *Anal. Chem.* **2000**, *72*, 3764-3770.
(2) Armistead, P. M.; Thorp, H. H. *Anal. Chem.* **2001**, *73*, 558-564.
(3) Yang, I. V.; Thorp, H. H. *Inorg. Chem.* **2000**, *39*, 4969-4976.
(4) Leone, A. M.; Weatherly, S. C.; Williams, M. E.; Thorp, H. H.; Murray, R. W. *J. Am. Chem. Soc.* **2001**, *123*, 218-222.
(5) Popovich, N. D. *IVD Technology* **2001**, *7*, 36-41.
(6) Baik, M.-H.; Silverman, J. S.; Yang, I. V.; Ropp, P. A.; Szalai, V. A.; Yang, W.; Thorp, H. H. *J. Phys. Chem. B* **2001**, *105*, 6537-6444.
(7) Williams, M. E.; Masui, H.; Long, J. W.; Malik, J.; Murray, R. W. *J. Am. Chem. Soc.* **1997**, *119*, 1997-2005.
(8) Dickinson, E., V; Williams, M. E.; Hendrickson, S. M.; Masui, H.; Murray, R. W. *J. Am. Chem. Soc.* **1999**, *121*, 613-616.
(9) Farrer, B. T.; Thorp, H. H. *Inorg. Chem.* **2000**, *39*, 44-49.

Appendices

Three copies of the following are attached:

Oxidation Kinetics of Guanine in DNA Molecules Adsorbed to Indium Tin Oxide Electrodes. P. M. Armistead, H. H. Thorp* *Anal. Chem.* **2001**, *73*, 558-564.

Kinetics of Metal-Mediated, One-Electron Oxidation of Guanine in Polymeric DNA and Oligonucleotides Containing Trinucleotide Repeat Sequences. I. V. Yang, H. H. Thorp* *Inorg. Chem.* **2000**, *39*, 4969-4976.

An Ionic Liquid Form of DNA: Redox-Active Molten Salts of Nucleic Acids. A. M. Leone, S. C. Weatherly, M. E. Williams, R. W. Murray*, H. H. Thorp* *J. Am. Chem. Soc.* **2001**, *123*, 218-222.

Oxidation Kinetics of Guanine in DNA Molecules Adsorbed onto Indium Tin Oxide Electrodes
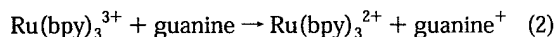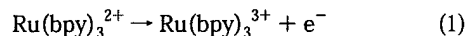
Paul M. Armistead and H. Holden Thorp*

Department of Chemistry and the Lineberger Comprehensive Cancer Center, University of North Carolina at Chapel Hill, Chapel Hill, North Carolina 27599-3290

Oligonucleotides containing the guanine nucleobase were adsorbed onto ITO electrodes from mixtures of DMF and acetate buffer. Chronocoulometry and chronoamperometry were performed on the modified electrodes in both phosphate buffer and buffer containing low concentrations of the inorganic complex $Ru(bpy)_3^{2+}$ (bpy = 2,2′ bipyridine), which catalyzes guanine oxidation. The charge and current evolution with and without the catalyst were compared to the charge and current evolution for electrodes that were treated with identical oligonucleotides that were substituted at every guanine with the electrochemically inert nucleobase hypoxanthine. Chronocoulometry over 2.5 s shows that roughly 2 electrons per guanine were transferred to the electrode in both the presence and absence of $Ru(bpy)_3^{2+}$, although at a slower rate for the uncatalyzed process. Chronoamperograms measured over 250 ms can be fit to a double exponential decay, with the intensity of the fast component roughly 6–20 times greater than that of the slow component. First- and second-order rate constants for catalytic and direct guanine oxidation were determined from the fast component. The maximum catalytic enhancement for immobilized guanine was found to be $i_{cat}/i_d = 4$ at 25 μM $Ru(bpy)_3^{2+}$. The second-order rate constant for the catalyzed reaction was 1.3×10^7 M^{-1} s^{-1}, with an apparent dissociation constant of 8.8 μM. When compared to parallel studies in solution, a smaller value of the dissociation constant and a larger value of the second-order rate constant are observed, probably due to distortion of the immobilized DNA, an increase in the local negative charge due to the oxygen sites on the ITO surface, and redox cycling of the catalyst, which maintains the surface concentration of the active form.

Oxidative damage of cellular DNA is currently viewed as a leading cause in disease processes as diverse as aging and cancer.[1–3] Because guanine is the most easily oxidized nitrogenous base, the chemical mechanism of its oxidation has been studied in detail.[4,5] While the mechanism of guanine oxidation in solution

has been well investigated, there have been very few mechanistic studies of guanine oxidation at the surface of an electrode. This information would be useful for the design of electrochemical nucleic acid biosensors based on the detection of guanine oxidation.[6–9] Specifically, it would be important to know how many electrons can be transferred to the electrode from each guanine base and the rate of that electron transfer. Previous solution electrochemistry studies have shown that uncatalyzed guanine electron transfer is slow at most electrode surfaces;[10] however, guanine oxidation has been observed when the guanine is adsorbed onto carbon paste electrodes.[9] In addition to base oxidation, many other electrochemical schemes for sensing DNA are being pursued.[11–16]

Our laboratory has developed a catalytic guanine oxidation system with the inorganic metal complex $Ru(bpy)_3^{2+}$ as the oxidation catalyst. Catalytic guanine oxidation proceeds through the following reactions[17]

$$Ru(bpy)_3^{2+} \rightarrow Ru(bpy)_3^{3+} + e^- \qquad (1)$$

$$Ru(bpy)_3^{3+} + guanine \rightarrow Ru(bpy)_3^{2+} + guanine^+ \qquad (2)$$

This reaction has been studied by digital simulation of solution electrochemistry and by stopped-flow spectroscopy.[17,18] Recently, we have developed a simple method for adsorbing DNA onto ITO electrodes that, when combined with the electrocatalytic scheme

(6) Napier, M. E.; Thorp, H. H. *Langmuir* **1997**, *13*, 6342–6344.
(7) Napier, M. E.; Loomis, C. R.; Sistare, M. F.; Kim, J.; Eckhardt, A. E.; Thorp, H. H. *Bioconjugate Chem.* **1997**, *8*, 906–913.
(8) Ontko, A. C.; Armistead, P. M.; Kircus, S. R.; Thorp, H. H. *Inorg. Chem.* **1999**, *38*, 1842–1846.
(9) Wang, J.; Bollo, S.; Paz, J. L. L.; Sahlin, E.; Mukherjee, B. *Anal. Chem.* **1999**, *71*, 1910–1913.
(10) Armistead, P. M.; Thorp, H. H. *Anal. Chem.* **2000**, *72*, 3764–3770.
(11) Millan, K. M.; Saraullo, A.; Mikkelsen, S. R. *Anal. Chem.* **1994**, *66*, 2943–2948.
(12) Wang, J.; Cai, X.; Rivas, G.; Shiraishi, H.; Farias, P. A. M.; Dontha, N. *Anal. Chem.* **1996**, *68*, 2629–2634.
(13) Kelley, S. O.; Boon, E. M.; Barton, J. K.; Jackson, N. M.; Hill, M. G. *Nucleic Acids Res.* **1999**, *27*, 4830–4837.
(14) Creager, S.; Yu, C. J.; Bamdad, C.; O'Connor, S.; MacLean, T.; Lam, E.; Chong, Y.; Olsen, G. T.; Luo, J.; Gozin, M.; Kayyem, J. F. *J. Am. Chem. Soc.* **1999**, *121*, 1059–1064.
(15) Singhal, P.; Kuhr, W. G. *Anal. Chem.* **1997**, *69*, 4828–4832.
(16) Xu, X.-H.; Bard, A. J. *J. Am. Chem. Soc.* **1995**, *117*, 2627–2631.
(17) (a) Johnston, D. H.; Glasgow, K. C.; Thorp, H. H. *J. Am. Chem. Soc.* **1995**, *117*, 8933–8938. (b) Sistare, M.; Holmberg, R.; Thorp, H. H. *J. Phys. Chem.* **1999**, *103*, 10718–10728.
(18) Yang, I. V.; Thorp, H. H. *Inorg. Chem.* **2000**, *39*, 4969–4976.

(1) Mecocci, P.; Fano, G.; Fulle, S.; MacGaverty, U.; Shinobu, L.; Polidori, M. C.; Cherubini, A.; Vecchiet, J.; Senin, U.; Flint Beal, M. *Free Radical Biol. Med.* **1999**, *26*, 303–308.
(2) Dreher, D.; Junod, A. F. *Eur. J. Cancer* **1996**, *32A*, 30–38.
(3) Loft, S.; Poulsen, H. E. *J. Mol. Med.* **1996**, *74*, 297–312.
(4) Burrows, C. J.; Muller, J. G. *Chem. Rev.* **1998**, *98*, 1109–1151.
(5) Steenken, S. *Chem. Rev.* **1989**, *89*, 503–520.

above, enabled us to detect DNA adsorbed onto ITO electrodes at surface densities as low as 44 amol/mm^2.[10] The adsorption procedure involves treatment of the electrodes with DNA dissolved in DMF/acetate, which is a denaturing medium and, therefore, leads to attachment of single-stranded DNA to the electrode. Because the detection system relies on oxidation of guanine, the modified electrodes can be interrogated on only one scan; in fact, we have shown previously that repeated scanning leads to a decrease in the catalytic current on successive scans.[10]

To probe the surface reaction in the electrocatalytic system, experiments were performed in which both direct oxidation of adsorbed guanine and Ru(bpy)$_3{}^{2+}$-catalyzed oxidation of adsorbed guanine could be monitored in the same experiment. In our previous studies, catalytic current enhancements were detected through cyclic voltammetry at fast scan rates (10 V s^{-1}).[10] In those experiments, guanine oxidation in the absence of catalyst was barely detectable, so the extent of catalysis could not be quantitatively evaluated. Here we report on chronocoulometry and chronoamperometry experiments on ITO electrodes that were treated with large amounts DNA of a specific sequence. These experiments were extended for much longer times (2.5 s), which allowed the slow direct guanine oxidation to be measured accurately. From these data, the number of electrons transferred to the electrode per guanine was quantified, and the rate constants for both the catalyzed and uncatalyzed reactions could be estimated. To obtain the kinetic information from the chrono-amperograms, a second term was added to the standard Cottrell equation. This term takes into account the catalytic reactions occurring near the electrode surface and accurately predicts the initial currents from such a reaction. This modification of the Cottrell equation potentially constitutes a general description of other electrochemical systems in which a scarce substrate is adsorbed onto the electrode surface and an electrocatalyst is present in the bulk solution.

EXPERIMENTAL SECTION

Materials and Reagents. Oligonucleotides were synthesized at the Lineberger Comprehensive Cancer Center Nucleic Acid Core Facility at the University of North Carolina. All water used was in-house distilled water that was further purified on a Milli-Q water purification system. N,N-Dimethyl formamide, sodium phosphate, sodium acetate, and sodium chloride were from Mallinckrodt (Paris, KY). [Ru(bpy)$_3$]Cl$_2$ was purchased as the chloride salt from Aldrich and was recrystallized from acetonitrile. ITO electrodes were purchased from Delta Technologies (Stillwater, MN). All electrochemical measurements were performed in a one-compartment cell on a BAS (Lafayette, IN) 100B potentiostat that was connected to a 200 MHz Pentium computer. A Ag/AgCl reference electrode from Cypress Systems was used (Lawrence, KS), and a platinum wire was used as an auxiliary electrode. All radiolabeling data were collected on a phosphorimager screen that was subsequently scanned on a Molecular Dynamics Storm 860 (San Jose, CA). Phosphorimager data analysis was performed using ImagQuaNT software.

Immobilization of DNA onto ITO Electrodes. Oligonucleotides containing the sequences 5′-AAA TAT (AGT)$_{20}$ ATA AAA (20G72), 5′-AAA TAT (AIT)$_{20}$ ATA AAA (20I72), and 5′-TTT TAT (ACT)$_{20}$ ATA TTT (20C72) were purified in 100 mM sodium acetate, pH = 6.8, on 3000 molecular-weight-cutoff filters. The

oligonucleotides were annealed by adding one volume of 20 μM oligonucleotide (either 20G72 or 20I72) to an equal volume of 20 μM 20C72. The solutions were heated to 95 °C for 5 min and allowed to slowly cool to room temperature. All experiments were performed on annealed samples, hereafter denoted as either 20G72 or 20I72.

ITO electrodes were cleaned by sonicating in Alconox (4 g/L) for 15 min; 2-propanol for 15 min; and Milli-Q water twice, for 15 min each.[19] The annealed DNA was added to 9 volumes of DMF, and 50 μL of the mixture were pipetted onto each cleaned ITO electrode. The electrodes were placed in a constant humidity chamber for 4 h. The electrodes were then immersed in different solutions that were agitated on a rotary mixer. The electrodes were first placed in water for 3 min; followed by 500 mM sodium chloride and 50 mM sodium phosphate, pH = 7.0, for 3 min; with three final water washes, each for 3 min. The electrodes were then allowed to air-dry. As we discussed in detail previously,[10] the adsorbed DNA is single-stranded, so treating the electrode with annealed DNA simply leads to the adsorption of both single strands in the duplex.

Quantification of DNA Adsorbed onto ITO Electrodes. Double-stranded 20G72 was 5′-labeled using T4 polynucleotide kinase (Life Technologies) and α-^{32}P ATP (Amersham). Briefly, 1 μL of 1 μM annealed oligonucleotide was added to 1 μL of α-^{32}P ATP, 1 μL of 5× forward reaction buffer, 1 μL of water, and 1 μL of kinase. The reaction was allowed to proceed at 37 °C for 15 min. The reaction was diluted to 70 μL by adding 65 μL of water. Unincorporated ATP was removed by passing the entire mix through a NucTrap purification column (Stratagene). The purified oligonucleotides were in a final volume of roughly 100 μL. From this volume, 1 μL was added to 100 μL of 10 μM annealed 20G72 in 100 mM sodium acetate, pH = 6.8. The doped sample was added to 9 volumes of DMF. The mixture was added to cleaned ITO electrodes and placed in a constant humidity chamber for 4 h. The electrodes were washed identically to nonradiolabeled ITO electrodes and allowed to air-dry. Quantification standards were produced by pipetting a 1-μL drop of the doped annealed solution (before addition of DMF) onto a piece of filter paper. The filter paper was dried and wrapped with the radiolabeled ITO electrodes in plastic wrap. The electrodes and standards were placed on a phosphorimager screen overnight. The screen was scanned on a Storm 860 phosphorimager, and analysis of the electrodes was performed using ImageQuaNT software.

Chronocoulometry of DNA Adsorbed onto ITO Electrodes. Solutions of annealed 10 μM 20G72 and 20I72 were prepared in 100 mM sodium acetate, pH = 6.8. The oligonucleotides were adsorbed, washed, and dried on cleaned ITO electrodes as described above. Chronocoulometry was performed with a double potential step from 900 to 1300 to 900 mV vs Ag/AgCl reference. A platinum wire was used as the auxiliary electrode. The step time was set at 2.5 s. Chronocoulometry was performed on ITO electrodes treated with 20G72 or 20I72 in 50 mM sodium phosphate buffer, pH = 7.0, in the presence or absence of 25 μM Ru(bpy)$_3{}^{2+}$. The $Q-t$ curve taken on electrodes treated with 20I72 was subtracted from the $Q-t$ curves taken on 20G72 electrodes.

(19) Willit, J. L.; Bowden, E. F. J. Phys. Chem. 1990, 94, 8241−8246.
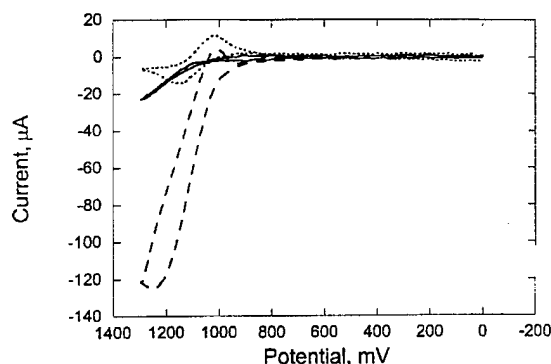
Figure 1. Cyclic voltammograms of calf thymus DNA-modified ITO electrodes at 10 V/s in the presence (dashed) and absence (solid) of 100 μM Ru(bpy)$_3^{2+}$. A cyclic voltammogram of 100 μM Ru(bpy) at an unmodified electrode is also shown (dotted).

Chronoamperometry of DNA Adsorbed onto ITO Electrodes. Chronoamperometry data were obtained by taking the derivative of chronocoulometry data. Solutions of annealed 10 μM 20G72 and 20I72 were prepared in 100 mM sodium acetate, pH = 6.8. The oligonucleotides were adsorbed, washed, and dried on cleaned ITO electrodes, as described above. Chronocoulometry was performed with a double potential step from 900 to 1300 to 900 mV vs Ag/AgCl reference. A platinum wire was used as the auxiliary electrode. The step time was set at 250 ms, and $Q-t$ curves were collected at varying concentrations of Ru(bpy)$_3^{2+}$ (0, 5, 10, 25, and 100 μM). For each Ru(bpy)$_3^{2+}$ concentration, 16 electrodes were modified with 20G72 and interrogated by chronocoulometry; the 16 $Q-t$ curves were averaged to generate a single $Q-t$ curve for that Ru(bpy)$_3^{2+}$ concentration. Similarly, 16 electrodes were modified with 20I72 for each Ru(bpy)$_3^{2+}$ concentration, interrogated by chronocoulometry, and averaged. The averaged $Q-t$ curve for each concentration for 20I72 was subtracted from the corresponding averaged $Q-t$ curve for 20G72. The derivative with respect to time was taken of the subtracted $Q-t$ curves, which yielded a chronoamperogram. These chronoamperomograms were fitted to double-exponentials shown in Figure 3.

RESULTS

Cyclic Voltammetry of Adsorbed DNA on ITO Electrodes. Previous electrochemical experiments on single-stranded DNA adsorbed onto ITO electrodes used cyclic voltammetry to measure catalytic oxidation of the adsorbed guanine bases. In these studies, electrocatalysis was measured by monitoring the increase in the Ru(bpy)$_3^{2+}$ oxidation wave in the cyclic voltammograms.[10] Although these experiments gave quantitative data on the nature of the electrocatalytic reaction being observed, the cyclic voltammograms did not yield any useful information on direct guanine oxidation in the absence of Ru(bpy)$_3^{2+}$.

Figure 1 shows representative cyclic voltammograms at 10 V/s of 100 μM Ru(bpy)$_3^{2+}$ at an unmodified ITO electrode, a DNA-modified electrode in the absence of Ru(bpy)$_3^{2+}$, and a DNA-modified electrode in a solution containing 100 μM Ru(bpy)$_3^{2+}$. The background charging current obtained from a bare ITO electrode in buffer was subtracted from all of the voltammograms. Direct DNA oxidation is only observable as a poorly defined
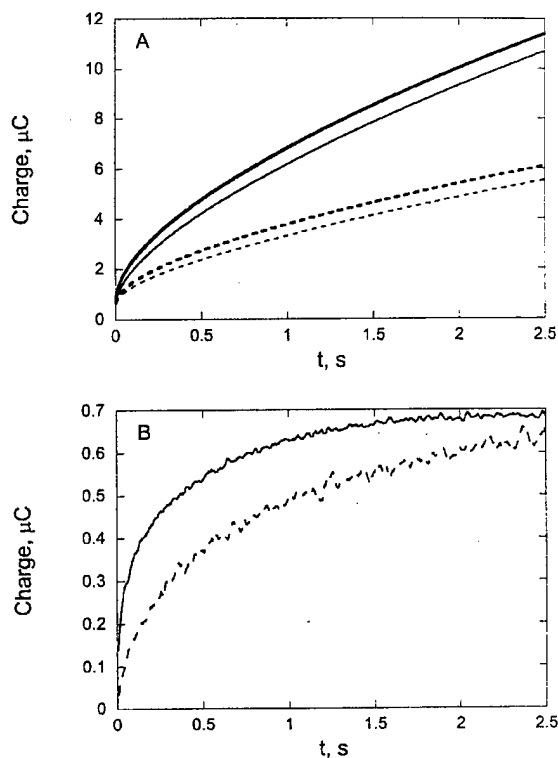
Figure 2. (A) $Q-t$ curves of electrodes modified with 20I72 or 20G72 (bold) with 25 μM Ru(bpy)$_3^{2+}$ (solid) or in buffer alone (dashed). (B) $Q-t$ curves of ITO electrodes treated with 20G72, minus the signals from the corresponding electrodes modified with 20I72 in 25 μM Ru(bpy)$_3^{2+}$ (solid) or in buffer (dashed).

oxidative wave with no peak, but there is a large catalytic enhancement in the oxidative wave for Ru(bpy)$_3^{2+}$. Detailed analysis of this phenomenon has been reported elsewhere.[17] As we have discussed, the cyclic voltammetry experiments provide the largest differences in absolute currents for the catalyzed and uncatalyzed reactions but do not allow for direct analysis of the extent of catalysis. Chronocoulometry and chronoamperometry were, therefore, used here under conditions of long times and high DNA loading to allow measurement of the slow, direct guanine oxidation and to quantify the catalytic rate enhancement due to Ru(bpy)$_3^{3+/2+}$. As we have discussed,[17] the rate of guanine oxidation can be a strong function of the secondary structure of the DNA; however, this effect is observed only at high salt concentration. At the low salt concentrations that was used here, the guanine oxidation rate is independent of the secondary structure;[18] thus, all of the guanines in the adsorbed DNA molecules contribute equally to the catalytic current observed in Figure 1.

Prior to electrochemical analysis of the reactions, we needed to know the precise quantity of DNA adsorbed to the electrodes, which was determined by analysis of electrodes that were modified with radiolabeled oligonucleotides using a phosphorimager. It was found that 180 fmol of DNA were adsorbed onto the 12.6 mm^2 electrodes. This value was further corrected to represent the number of moles of guanine present. Because each duplex used to treat the electrode contained 20 guanines, the total amount of guanine sampled during an electrochemical measurement was 3.7
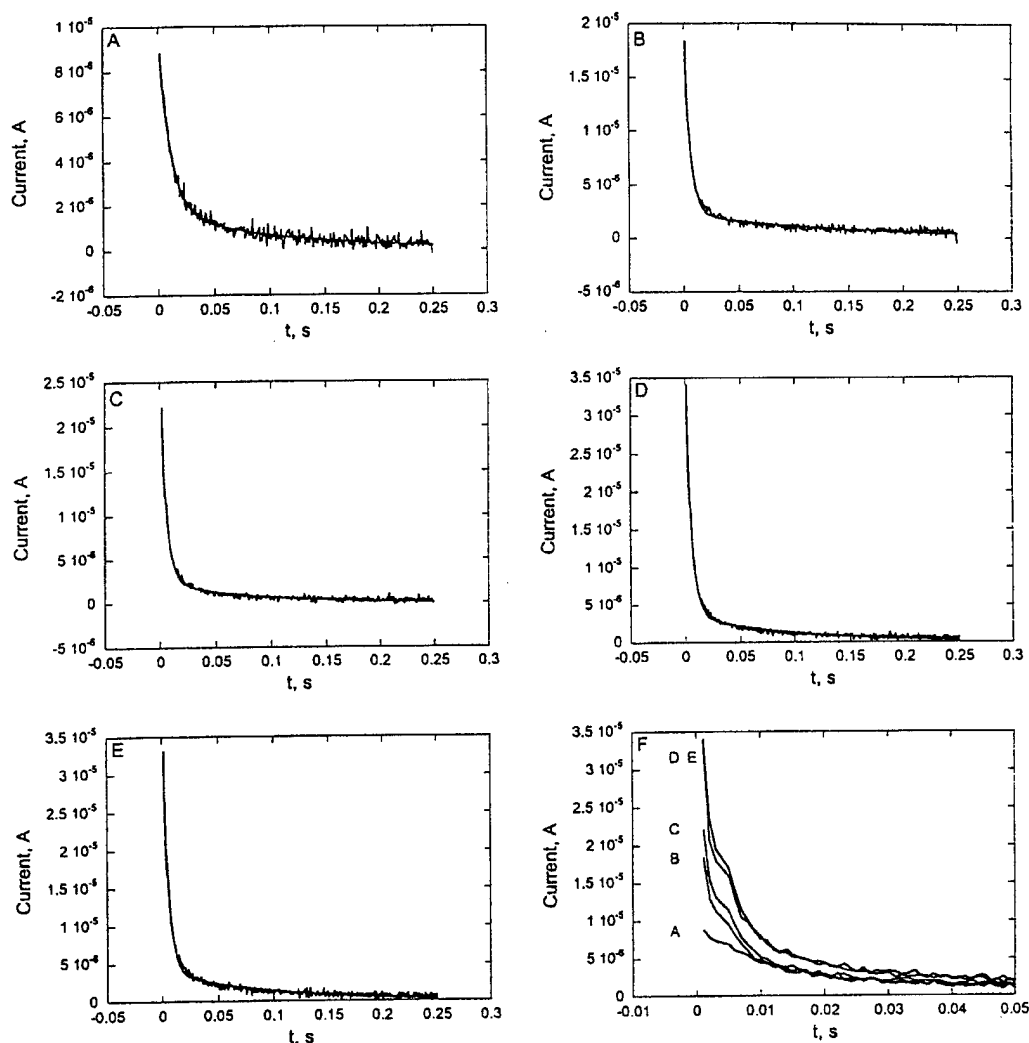
Figure 3. Chronoamperomograms of 20G72 taken at 0, 5, 10, 25, and 100 μM Ru(bpy)$_3^{2+}$, minus data for 20I72 at the same Ru(bpy)$_3^{2+}$ concentrations (panels A–E, respectively). Each chronoamperomogram was generated from 16 20G72 and 16 20I72 electrodes; see Experimental Section. Chronoamperomograms were generated by taking the derivative of the corresponding Q–t curve. Each trace was fit to a double exponential curve. Panel F shows all five traces overlaid; note the difference in time axis for panel F.

± 1.1 pmol (representing an average over six measurements). Note that the oligonucleotides used in this study were annealed to their complements prior to adsorption onto the electrodes; however, later experiments showed that the adsorbed molecules were single-stranded.[10] Thus, the electrode modifications carried out here simply produced equal amounts of each single strand immobilized to the electrode.

Chronocoulometry of Adsorbed DNA. Although ITO electrodes exhibit very small water oxidation currents, simple background subtraction was still needed to detect low levels of catalysis. The background subtraction was performed using electrodes that had 20I72 adsorbed onto the ITO in the same manner as 20G72. The hypoxanthine base is electrochemically inert at guanine oxidation potentials,[7] so subtraction of signals due to 20I72 accurately reflects the effects of electrode poisoning without artificially reducing the amount of charge transferred from guanine. When electrodes modified with 20G72 and 20I72 were interrogated by cyclic voltammetry, large current enhancements were observed with 20G72 (as in Figure 1), but the signals for

electrodes modified with 20I72 were identical to those for Ru(bpy)$_3^{2+}$ alone. As a further control, electrodes were modified with analogues of 20I72 where all of the hypoxanthines were changed to thymine. These electrodes gave currents identical to those from electrodes modified with 20I72. Thus, using 20I72-modified electrodes as a background also allowed any minor charge contributions from the other bases to be effectively subtracted.

Figure 2A shows unsubtracted chronocoulometry traces over 2.5 s for both 20G72- and 20I72-modified electrodes with and without Ru(bpy)$_3^{2+}$. If the 20I72 trace from Figure 2A is subtracted from the 20G72 trace made at the same concentration of Ru(bpy)$_3^{2+}$, a charge vs time plot can be drawn that reflects the charge transfer due solely to guanine oxidation. These plots are shown in Figure 2B for both the uncatalyzed (0 μM Ru(bpy)$_3^{2+}$) and catalyzed (25 μM Ru(bpy)$_3^{2+}$) reactions. At sufficiently long times, the same amount of charge is transferred from guanine to the electrode with and without Ru(bpy)$_3^{2+}$. The number of electrons transferred per guanine, n, can be determined using the Faraday relation

$$Q = nFm \qquad (3)$$

where Q is the charge, F is the Faraday constant (96,485 C mol^{-1}), and m is the number of moles of guanine. By combining data from the radiolabeled experiments with chronocoulometry, it was found that 1.9 ± 0.6 electrons per guanine were transferred to the electrode. A similar value of 2.2 ± 0.4 electrons per guanine was determined from integration of cyclic voltammograms in our previous study.[10] A two-electron oxidation is readily accounted for by a number of proposed oxidation mechanisms.[20-25]

Chronoamperometry of Adsorbed DNA on ITO. To gain a more quantitative understanding of the extent to which Ru(bpy)$_3^{2+}$ catalyzes guanine electron transfer, analysis of guanine oxidation currents was performed at various Ru(bpy)$_3^{2+}$ concentrations. Chronocoulometry was performed with 250-ms step-times on electrodes that were treated with either 20G72 or 20I72. These measurements were performed with Ru(bpy)$_3^{2+}$ concentrations of 0, 5, 10, 25, and 100 μM. The Q–t curves of the 20I72-treated electrodes were subtracted from those for the 20G72-treated electrodes, and the derivatives with respect to time of the subtracted Q–t curves were taken.

The current vs time traces obtained from the subtraction procedure are shown for varying Ru(bpy)$_3^{2+}$ concentrations in Figure 3. The guanine oxidation current drops off rapidly (within 30 ms) for all of the electrodes; however, the most rapid drop and the greatest initial oxidation current occurs at higher Ru(bpy)$_3^{2+}$ concentrations. The initial currents at each Ru(bpy)$_3^{2+}$ concentration are shown in Figure 4A and show that catalyzed guanine electron transfer is roughly 4 times faster than the uncatalyzed reaction under these conditions. The initial current from guanine oxidation at 25 μM Ru(bpy)$_3^{2+}$ is 34 μA, but at 0 μM, the initial current is 7.7 μA. The initial currents from Figure 4A begin to plateau at higher Ru(bpy)$_3^{2+}$ concentrations, which suggests the saturation of a binding preequilibrium. The initial currents from Figure 4A were normalized so that current from direct guanine oxidation [at 0 μM Ru(bpy)$_3^{2+}$] was zero. These data points were then fit to a standard binding isotherm

$$i = \frac{i_{max}[\text{Ru(bpy)}_3^{2+}]}{[\text{Ru(bpy)}_3^{2+}] + K_D} \qquad (4)$$

where i_{max} is the maximum current obtained and K_D is the apparent dissociation constant for Ru(bpy)$_3^{3+}$ and the immobilized DNA. As described below, we can assume that the concentration of Ru(bpy)$_3^{3+}$ at the surface is the same as the concentration of Ru(bpy)$_3^{2+}$ in the bulk, so the concentration of Ru(bpy)$_3^{2+}$ is used in eq 4. From this curve, a value of $K_D = 8.8 \pm 3.7$ μM was determined.

(20) Hickerson, R. P.; Prat, F.; Muller, J. G.; Foote, C. S.; Burrows, C. J. *J. Am. Chem. Soc.* **1999**, *121*, 9423–9428.

(21) Arkin, M. R.; Stemp, E. D. A.; Pulver, S. C.; Barton, J. K. *Chem. Biol.* **1997**, *4*, 389–400.

(22) Cullis, P. M.; Malone, M. E.; Mreson-Davis, L. A. *J. Am. Chem. Soc.* **1996**, *118*, 2775–2781.

(23) Muller, J. G.; Duarte, V.; Hickerson, R. P.; Burrows, C. J. *Nucleic Acids Res.* **1998**, *26*, 2247–2249.

(24) Duarte, V.; Muller, J. G.; Burrows, C. J. *Nucleic Acids Res.* **1999**, *27*, 496–502.

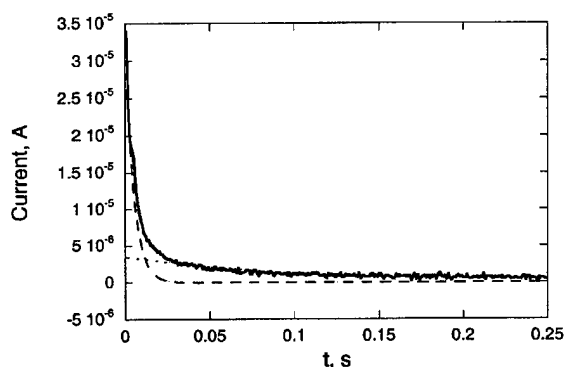(25) Kino, K.; Saito, I.; Sugiyama, H. *J. Am. Chem. Soc.* **1998**, *120*, 7373–7374.
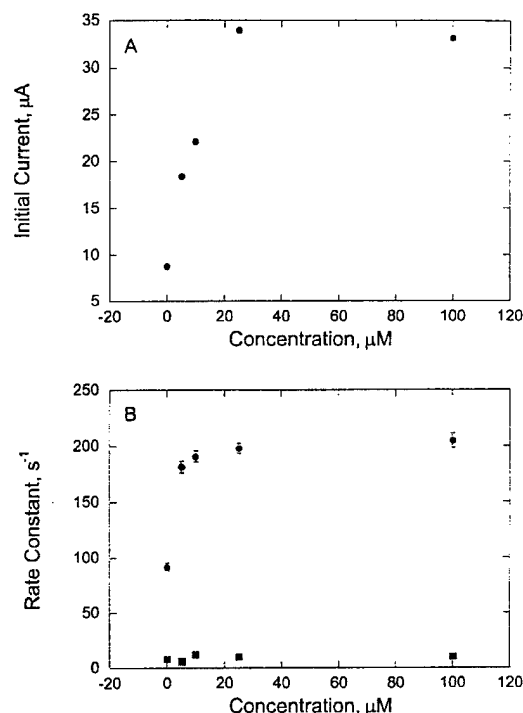
Figure 4. (A) Plot of the initial currents at each concentration of Ru(bpy)$_3^{2+}$, determined from the current vs time traces shown in Figure 3. (B) Plot showing both the fast (●) and slow (■) exponential terms from each double exponential fit of the traces in Figure 3. The error bars were determined from the fit of each trace (16 trials per concentration).

The current vs time traces in Figure 3 did not follow a simple $t^{1/2}$ dependence that would be expected for diffusion controlled-process.[26] Instead, the curves could be fit to double-exponential functions [i.e., $A_1 \exp(-k_1 t) + A_2 \exp(-k_2 t)$]. The rate constants for both the fast and slow components are shown in Figure 4B. In all of the fits, the fast component was 10–20 times more intense than the slow component (i.e., $A_1/A_2 > 10$). In addition, the slow component does not vary with the Ru(bpy)$_3^{2+}$ concentration, but the fast component increases with increasing Ru(bpy)$_3^{2+}$ concentrations and reaches a maximum value of 205 s^{-1} at 100 μM Ru(bpy)$_3^{2+}$. Figure 5 shows the total decay curve, with both the fast and slow components illustrated, for 25 μM Ru(bpy)$_3^{2+}$. The fast component dominates the current trace for the first 15 ms of the reaction. Because of its low intensity and lack of variation with Ru(bpy)$_3^{2+}$ concentration, the slow component was not analyzed further.

DISCUSSION

Catalytic Current Analysis. Kinetic analysis of electrocatalysis has typically been limited to the study of systems in which the substrate is in solution and the catalyst is either in solution or immobilized on the electrode surface. These types of systems have shown great utility in the detection of both small molecule and biomolecule analytes.[27,28] In an electrochemical detection system

(26) Bard, A. J.; Faulkner, L. R. *Electrochemical Methods*, 2nd ed.; John Wiley and Sons: New York, 1980.

(27) Pikulski, M.; Gorski, W. *Anal. Chem.* **2000**, *72*, 2696–2702.

(28) Wilkins, E.; Atanasov, P. *Med. Eng. Phys.* **1996**, *18*, 273–288.

$$DNA_s + [Ru(bpy)_3^{3+}]_{x=0} \xrightarrow{k} DNA_{s,ox} + [Ru(bpy)_3^{2+}]_{x=0} \quad (7)$$

where k is the second-order rate constant ($M^{-1} s^{-1}$), DNA_s is the adsorbed DNA, and $DNA_{s,ox}$ is the adsorbed DNA in which the guanine has been oxidized by one electron. The electrochemical reaction proceeds by diffusion control (see eq 1) and retains the interfacial concentrations of the solution species, that is, [Ru(bpy)_3^{3+}]_{x=0} = $C_{red,bulk}$ and [Ru(bpy)_3^{2+}]_{x=0} = 0 (eqs 6 and 7). Thus, there will be an additional current, $i_{surface}$, affected by reaction 7, for which

$$i_{surface} = -FA\frac{d\Gamma_{red}}{dt} = FAk\Gamma_{red}[Ru(bpy)_3^{3+}]_{x=0} =$$
$$FAk\Gamma_{red}C_{red,bulk} = FAK'\Gamma_{red} \quad (8)$$

where K' ($= kC_{red,bulk}$) is the effective pseudo-first-order rate constant, and Γ_{red} (mol/cm^2) is the surface concentration of the oxidizable units. Equation 8 gives

$$i_{surface} = FAK'\Gamma_T e^{-K't} \quad (9)$$

where Γ_T is the amount of guanine initially present on the electrode surface, that is, the total amount of guanine on the electrode surface. Then, the total current for the redox process is[30]

$$i_{total} = i_{Cottrell} + i_{surface} = FA\left[\frac{\sqrt{D}C_{red,bulk}}{\sqrt{\pi t}} + K'\Gamma_T e^{-K't}\right] \quad (10)$$

where $\Gamma_T = \Gamma_{red} + \Gamma_{ox}$. According to eq 10, the kinetic current is maximized compared to the Cottrell current when $t = 1/2 k'$. To analyze the kinetic current directly, we use eq 9, where Γ_T is approximately equal to the surface concentration of guanine in mol/cm^2.

Comparison of Rate Constants. Equation 9 was used to determine the rate constants for the fast component in Figure 4B. At high ruthenium concentrations (100 μM), the measured rate constant describes the electron transfer via a guanine·Ru(bpy)_3^{3+} complex. At lower ruthenium concentrations, the observed rate constant contains contributions from both direct guanine oxidation and oxidation via the guanine·Ru(bpy)_3^{3+} complex. As the ruthenium concentration decreases, the contribution from direct guanine oxidation increases, resulting in an overall decrease in the observed first-order rate constant. The observed first-order rate constant for adsorbed guanine at 0 μM Ru(bpy)_3^{2+} (92 s^{-1}) describes the uncatalyzed first-order electron-transfer reaction of guanine to the electrode. Thus, the maximum rate constant of 205 s^{-1} is likely a sum of the uncatalyzed and catalyzed rates, giving a rate for the catalyzed electron transfer of 110 s^{-1}. With a $K' = 205$ s^{-1}, the optimal time for measuring the kinetic current from eq 6 is 2.5 ms, which is near the time resolution of the present experiment, but provides support for analyzing the reaction at the earliest possible times, which we have done here.

Figure 5. Current vs time plot taken at 25 μM Ru(bpy)_3^{2+} (solid) showing the slow (dotted) and fast (dashed) components from the double-exponential fit.

in which the analyte is the scarce component to be detected (e.g., a large biomolecule), attachment of the analyte to the electrode surface increases its surface concentration and hence the sensitivity.[29] The catalytic DNA oxidation reaction described here involves the adsorption of a scarce analyte and the use of a solution-bound electrocatalyst, Ru(bpy)_3^{2+}. Our goal here was to observe both the catalyzed and uncatalyzed oxidations using the same technique, which was possible only with high DNA loadings and on long time scales with chronocoulometry. Under these conditions, the rate enhancements provided by the redox couple were modest; however, the results in Figure 1 show that much larger catalytic effects are apparent with cyclic voltammetry. Detailed analysis of the results in Figure 1 is not possible, due to the poor resolution of the uncatalyzed reaction.

Oxidation of Ru(bpy)_3^{2+} in solution at a bare electrode (or one with adsorbed inosine) yields a normal chronamperogram. When the potential is such that the concentration of reduced ruthenium at the electrode is zero (i.e., [Ru(bpy)_3^{2+}]_{x=0} = 0), the diffusion-controlled current response for such a system is described by the Cottrell equation[26]

$$i_{Cottrell} = FA\left(\frac{\sqrt{D}C_{red,bulk}}{\sqrt{\pi t}}\right) \quad (5)$$

where i is the current, n is the number of electrons transferred in the process, A is the electrode area, D is the diffusion coefficient of the electroactive species, and $C_{red,bulk}$ is the concentration of the electroactive species in solution. Under these conditions, we can also write that

$$C_{ox,x=0} = C_{red,bulk}\sqrt{\frac{D_{ox}}{D_{red}}} \cong C_{red,bulk} \quad (\text{if } D_{ox} = D_{red}) \quad (6)$$

where $C_{ox,x=0} = [Ru(bpy)_3^{3+}]_{x=0}$ and D_{ox} and D_{red} are the diffusion coefficients of Ru(bpy)_3^{2+} and Ru(bpy)_3^{3+}, respectively. Thus, [Ru(bpy)_3^{3+}]_{x=0} is maintained at a constant concentration at the electrode surface. The adsorbed species, which is electrochemically inert, can react with the Ru(bpy)_3^{3+} according to

---

(29) Palecek, E. *Electroanalysis* **1996**, *8*, 7–14.

(30) Feldberg, S. W., personal communication.

The understanding developed through analysis of the first-order rate constant and the binding isotherm provides a strong basis for the large current enhancements that are seen in cyclic voltammetry (Figure 1 and ref 10). The first-order rate constant of 110 s^{-1} is somewhat larger than the corresponding first-order rate constants determined for electron transfer within the Ru-(bpy)$_3^{3+}$·DNA complex in solution.[17b] In the solution cases, the first-order rate constants were about 30 s^{-1} for similar sequences and conditions. Thus, the DNA–Ru^{3+} electron transfer at the surface is similar to that in solution. The somewhat faster electron-transfer rate observed at the surface is likely due to a distortion of the immobilized DNA that increases the solvent accessibility of the oxidized guanine.

The surface immobilization has a much larger effect on the affinity of the catalyst for DNA than on the electron-transfer rate. In solution, Ru(bpy)$_3^{3+}$ binds to DNA with a dissociation constant of about 1 mM,[31] and the apparent affinity at the electrode surface is 8.8 μM, as determined from eq 4. This 100-fold increase in affinity is likely due to partial negative charges on the ITO surface,[32] which increase the electrostatic attraction of the cationic catalyst to the DNA-modified ITO surface. In addition, there is likely an increase in the *apparent* affinity arising from the redox cycling of the catalyst, which imposes a large driving force for accumulation of Ru(bpy)$_3^{3+}$ at the electrode surface. This driving force arises because the electrode is poised at potentials capable of oxidizing Ru(bpy)$_3^{2+}$, while reduction by the adsorbed DNA is simultaneously suppressing the surface concentration of Ru-(bpy)$_3^{3+}$.

CONCLUSIONS

Oxidation of an adsorbed analyte by a solution-based electrocatalyst provides a potential solution to the direct detection of a native biomolecule.[33] In such a system, adsorption of the analyte increases its effective concentration, but addition of the solution-based catalyst increases the rate of electron transfer, which is often slow for biomolecules.[27] We have described here the kinetic analysis for such a system in which DNA is adsorbed onto ITO electrodes, and Ru(bpy)$_3^{3+/2+}$ is used to increase the rate of electron transfer from guanines in DNA to the electrode surface. The particular system discussed is one in which the DNA molecules are single-stranded and oriented parallel to the ITO surface. In this configuration, the electrogenerated Ru(bpy)$_3^{3+}$ is reduced back to Ru(bpy)$_3^{2+}$ at the electrode surface, prohibiting the diffusion of Ru(bpy)$_3^{3+}$ away from the electrode surface at short times. The kinetics of this scenario are described by a modification to the Cottrell equation that accounts for both the diffusive current, giving a $t^{1/2}$ dependence, and a catalytic current, which gives an e^{-kt} dependence. The contribution to the catalytic current is, therefore, maximized at early times.

Although the present system does not allow for flux of Ru-(bpy)$_3^{3+}$ away from the electrode surface, such a system could be designed using an intervening layer that would position the DNA at some larger distance from the electrode, such that reduction of Ru(bpy)$_3^{3+}$ immediately at the electrode surface would not occur. In such a system, additional terms would need to be added to eq 10 to describe the catalytic reaction in solution.[34] Ordinarily, detection of catalytic current for solution reactions is limited to electrodes large enough to exhibit planar diffusion;[35-37] however, systems described by eq 6 would not be subject to this limitation. Thus, systems such as that described here might allow for further miniaturization of the detection electrode and, hence, to greater sensitivity.

(31) Johnston, D. H.; Thorp, H. H. *J. Phys. Chem.* **1996**, *100*, 13837–13843.
(32) *Oxides and Oxide Films*; Ahmed, S. M., Ed.; Marcel Dekker: New York, 1972; Vol. 1, pp 320–402.
(33) Thorp, H. H. *Trends Biotechnol.* **1998**, *16*, 117–121.
(34) Nicholson, R. S.; Shain, I. *Anal. Chem.* **1964**, *36*, 706–735.
(35) Heinze, J. *Ber. Bunsen-Ges. Phys. Chem.* **1981**, *85*, 1096–1103.
(36) Dayton, M. A.; Ewing, A. G.; Wightman, R. M. *Anal. Chem.* **1980**, *52*, 2392–2396.
(37) Szalai, V. A.; Thorp, H. H. *J. Phys. Chem. B* **2000**, *104*, 6851–6859.

Kinetics of Metal-Mediated One-Electron Oxidation of Guanine in Polymeric DNA and in Oligonucleotides Containing Trinucleotide Repeat Sequences

Ivana V. Yang and H. Holden Thorp*

Department of Chemistry, The University of North Carolina, Chapel Hill, North Carolina 27599-3290

Received June 6, 2000

The oxidation of guanines in DNA by Ru(III) is investigated by catalytic electrochemistry and stopped-flow spectrophotometry. The reactions of calf thymus DNA (20% guanine) and herring testes DNA (25% guanine) with $Ru(bpy)_3^{3+}$ (bpy = 2,2'-bipyridine) show biexponential decays in stopped-flow spectrophotometric experiments with the fast and slow components in 2:1 ratios and average rate constants in 880 mM NaCl of $\langle k \rangle = 18\ 700\ M^{-1}$ s^{-1} for calf thymus DNA and $\langle k \rangle = 24\ 600\ M^{-1}\ s^{-1}$ for herring testes DNA. The higher rate constant for the more guanine-rich DNA is possibly due to a higher density of electron-rich guanine multiplets. The observation of a biexponential decay is incorporated into digital simulations of the catalytic voltammograms observed for Ru-$(bpy)_3^{2+}$ in the presence of DNA. For both DNAs, the rates observed by voltammetry are somewhat slower than those observed by stopped-flow spectrophotometry and the dependence of the rate constants on scan rate using the biexponential model is less pronounced than when only one decay is treated, supporting the notion that the scan rate dependence arises from the multiphasic decay. At low salt concentrations, where binding of the metal complex to DNA increases the effective catalytic rate constant, rates can be measured by stopped-flow spectrophotometry only with a less oxidizing complex, $Fe(bpy)_3^{3+/2+}$, which yields trends in the rate constants similar to those observed for the case of $Ru(bpy)_3^{3+/2+}$ at high ionic strength. Oligonucleotides based on the trinucleotide repeat sequences $(AGT)_n$ and $(GAA)_n$ produce significant catalytic currents, which are readily interpreted in terms of the guanine concentration and the secondary structure discerned from gel electrophoresis experiments. These experiments may provide a basis for sensing secondary structures and repeat numbers in biologically relevant DNAs.

Introduction

Electrochemistry offers an attractive approach to genetic analysis for a number of reasons that have been previously discussed.[1–16] A challenge in developing electrochemical methods for nucleic acid analysis is the identification of the appropriate redox-active moiety to analyze. For direct analysis, oxidation of the nucleic acid bases is the most facile; however, the potentials required for these reactions are high and generally near those where most electrodes oxidize water.[11,13] Other electrochemical approaches center on detection of exogenous redox labels that either interact specifically with double-stranded DNA[3–5,7–9,12,14–16] or are covalently attached to the target nucleic acid.[1,2,6,10]
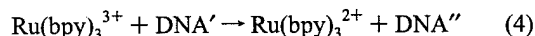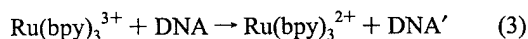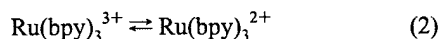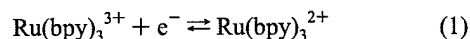
We have described an electrochemical approach to nucleic acid analysis where DNA sequence and structure are probed by $Ru(bpy)_3^{2+}$-mediated oxidation of guanine nucleobases ($E_{1/2}[Ru(III/II)] = 1.06$ V and $E_{1/2}[G(1+/0)] \sim 1.1$ V vs Ag/AgCl).[17–19] This method is based on the detection of current enhancement in the cyclic voltammogram of $Ru(bpy)_3^{2+}$ measured at indium tin oxide (ITO) electrodes in the presence of DNA (bpy = 2,2'-bipyridine). The large number of guanine bases present in polymeric DNA combined with the use of miniaturized electrodes may allow detection of small amounts of genomic DNA fragments. In fact, we recently reported detection of immobilized DNA on ITO electrodes at a density of only 44 amol/mm².[20] This method is attractive because the ITO electrodes do not oxidize water or guanine significantly at the potential where the $Ru(bpy)_3^{3+/2+}$ couple occurs and the rate constant for $Ru(bpy)_3^{3+}$-guanine electron transfer is ex-

(1) Caruana, D. J.; Heller, A. *J. Am. Chem. Soc.* **1999**, *121*, 769−774.
(2) Hartwich, G.; Caruana, D. J.; deLumley-Woodyear, T.; Wu, Y.; Campbell, C. N.; Heller, A. *J. Am. Chem. Soc.* **1999**, *121*, 10803−10812.
(3) Hashimoto, K.; Ito, K.; Ishimori, Y. *Anal. Chem.* **1994**, *66*, 3830−3833.
(4) Kelley, S. O.; Barton, J. K.; Jackson, N. M.; Hill, M. G. *Bioconjugate Chem.* **1997**, *8*, 31−37.
(5) Kelley, S. O.; Boon, E. M.; Barton, J. K.; Jackson, N. M.; Hill, M. G. *Nucleic Acids Res.* **1999**, *27*, 4830−4837.
(6) Korri-Youssoufi, H.; Garnier, F.; Srivastava, P.; Godillot, P.; Yassar, A. *J. Am. Chem. Soc.* **1997**, *119*, 7388−7389.
(7) Marrazza, G.; Chianella, I.; Mascini, M. *Biosens. Bioelectron.* **1999**, *14*, 43−51.
(8) Millan, K. M.; Mikkelsen, S. R. *Anal. Chem.* **1993**, *65*, 2317−2323.
(9) Millan, K. M.; Saraullo, A.; Mikkelsen, S. R. *Anal. Chem.* **1994**, *66*, 2943−2948.
(10) O'Connor, S. D.; Olsen, G. T.; Creager, S. E. *J. Electroanal. Chem. Interfacial Electrochem.* **1999**, *466*, 197−202.
(11) Palecek, E.; Fojta, M. *Anal. Chem.* **1994**, *66*, 1566−1571.
(12) Takenaka, S.; Yamashita, K.; Takagi, M.; Uto, Y.; Kondo, H. *Anal. Chem.* **2000**, *72*, 1334−1341.
(13) Wang, J.; Rivas, G.; Fernandes, J. R.; Paz, J. L. L.; Jiang, M.; Waymire, R. *Anal. Chim. Acta* **1998**, *375*, 197−203.
(14) Wang, J.; Fernandes, J. R.; Kubota, L. T. *Anal. Chem.* **1998**, *70*, 3699−3702.
(15) Xu, X.-H.; Yang, H. C.; Mallouk, T. E.; Bard, A. J. *J. Am. Chem. Soc.* **1994**, *116*, 8386-8387.
(16) Xu, X.-H.; Bard, A. J. *J. Am. Chem. Soc.* **1995**, *117*, 2627−2631.

(17) Johnston, D. H.; Thorp, H. H. *J. Phys. Chem.* **1996**, *100*, 13873−13843.
(18) Johnston, D. H.; Glasgow, K. C.; Thorp, H. H. *J. Am. Chem. Soc.* **1995**, *117*, 8933−8938.
(19) Steenken, S.; Jovanovic, S. V. *J. Am. Chem. Soc.* **1997**, *119*, 617−618.
(20) Armistead, P. M.; Thorp, H. H. *Anal. Chem.* **2000**, *72*, 3764−3770.

tremely large, approaching 10^6 M^{-1} s^{-1}.[21] Accordingly, large current enhancements are obtained for micromolar concentrations of Ru(bpy)$_3$$^{2+}$ even when the DNA concentration is less than that of the catalyst.[21]

We have utilized the cyclic voltammetry simulation program DigiSim[22] to analyze the catalytic mechanism and extract rate constants for guanine oxidation in different DNA environments.[17,18,21] A relatively simple mechanism can be used for the case at high ionic strength where binding of the metal complex to DNA can be neglected:

$$Ru(bpy)_3^{3+} + e^- \rightleftharpoons Ru(bpy)_3^{2+} \qquad (1)$$

$$Ru(bpy)_3^{3+} \rightleftharpoons Ru(bpy)_3^{2+} \qquad (2)$$

$$Ru(bpy)_3^{3+} + DNA \rightarrow Ru(bpy)_3^{2+} + DNA' \qquad (3)$$

$$Ru(bpy)_3^{3+} + DNA' \rightarrow Ru(bpy)_3^{2+} + DNA'' \qquad (4)$$

Here DNA′ is a DNA molecule where one electron has been removed from guanine and DNA″ is a DNA molecule where two electrons have been removed from guanine. The mechanism accounts for slow spontaneous conversion of the oxidized metal complex back to the reduced form (eq 2), which is known to occur at neutral pH.[23] The mechanism also provides for DNA overoxidation (eq 4), since many guanine oxidation products are more easily oxidized than guanine itself.[24] At high salt concentration, the rate constant for oxidation of guanine in calf thymus DNA (eq 3) is ~1×10^4 M^{-1} s^{-1} according to cyclic voltammetry; this value has been confirmed independently by pulsed voltammetry, chronoamperometry, and stopped-flow spectrophotometry.[18]

At low ionic strength, electrostatic binding of the mediator to the nucleic acid increases the catalytic current enhancement and accelerates the rate of guanine oxidation by an order of magnitude. This binding equilibrium complicates the mechanism, however, because square schemes accounting for bound and free ruthenium must be added for each electron transfer.[17] In addition, chronoamperometry studies have shown that, at low salt concentrations, the reaction exhibits biphasic kinetics with rates that differ by roughly an order of magnitude.[21] The biphasic nature of the reaction is also apparent in the scan rate dependence of the rate constants obtained from cyclic voltammetry. We have shown that the Λ and Δ enantiomers of Ru(bpy)$_3$$^{2+}$ oxidize guanine with similar rates, eliminating the possibility that the biphasic kinetics are a result of the stereoisomerism of the metal complex.[21]

We now extend our studies to Ru(bpy)$_3$$^{2+}$-mediated oxidation of polymeric and oligomeric DNAs containing different numbers of guanines. The primary question we address is whether the scan rate dependence from cyclic voltammetry is apparent as biphasic kinetics in homogeneous reactions that do not involve a solid electrode. This question was investigated by performing parallel studies of the oxidations of polymeric and oligonucleotide DNAs by stopped-flow spectrophotometry and cyclic voltammetry. A consistent model has been developed for analyzing both kinds of kinetic data where the stopped-flow results can be used to guide the electrochemical analysis. We

also address three additional questions. First, what is the effect of changing the density of guanine in each strand of DNA? Second, how do noncanonical DNA structures affect the electrochemical response and apparent rate constant? Finally, since samples such as calf thymus DNA contain many sequences and fragment lengths, what is the role of polydispersity in the DNA sample? These questions have been addressed by studying the reactions of genomic DNAs from calf thymus and herring testes, which have different percentages of guanine (20% and 25%, respectively).[25] In addition, we have studied monodisperse oligonucleotides consisting of triplet repeats that contain a single guanine; such sequences are relevant to the disease-causing trinucleotide expansions that occur in genomic DNAs.[26-28]

Experimental Section

Materials. Calf thymus and herring testes DNA samples were purchased from Sigma and sheared by repeated sonication and passage through a 22-gauge needle.[29] Synthetic oligonucleotides were purchased from the Nucleic Acid Core Facility at the Lineberger Comprehensive Cancer Center of The University of North Carolina at Chapel Hill and purified on Microcon YM-3 centrifugal filters (Millipore). Water was purified with a Milli-Q purification system (Millipore). Salts for buffer preparation were purchased from Mallinckrodt, and ligands and metal salts were purchased from Aldrich. Published procedures were used to prepare the metal complexes [Ru(bpy)$_3$]Cl$_3$, [Fe(bpy)$_3$]Cl$_3$,[30] and [Os(bpy)$_2$(dppz)]Cl$_2$,[31] (bpy = 2,2′-bipyridine, dppz = dipyridophenazine). Gel electrophoresis reagents (acrylamide, agarose, TBE buffer) were purchased from Bio-Rad. All solution concentrations were determined spectrophotometrically using a Hewlett-Packard HP 8452 diode array spectrophotometer and known extinction coefficients.[18,31,32] Extinction coefficients for oligonucleotides were calculated using the nearest-neighbor equation,[33] giving the concentration of nucleic acid in strand concentration. Solutions of double-stranded oligonucleotide were prepared by mixing 1:1.2 guanine-containing and complementary oligonucleotides in the desired buffers, heating at 90 °C for 5 min, and cooling the mixtures to room temperature over a period of 3 h.

Stopped-Flow Spectrophotometry. Kinetic experiments were carried out using an On Line Instrument Systems RSM-1000 stopped-flow spectrophotometer. The reactions were monitored spectrophotometrically from 350 to 580 nm for 2.0 s at 1000 scans/s for Ru(bpy)$_3$$^{3+}$ and for 5 min at 21 scans/s for Fe(bpy)$_3$$^{3+}$. Solutions were maintained at 25 ± 1 °C. M(bpy)$_3$$^{3+}$ (M = Ru, Fe) and DNA were dissolved in ~10 mM H$_2$SO$_4$ (pH 2) and pH 8 phosphate buffer, respectively, and these solutions were then mixed to give a solution that was 50 mM in sodium phosphate, pH 7, with or without 800 mM NaCl after mixing. Concentrations of Ru(bpy)$_3$$^{2+}$ and Fe(bpy)$_3$$^{3+}$ in each run were obtained from A_{min} and $A_{max}-A_{min}$ at 452 nm (ϵ = 14 600 M^{-1} cm^{-1}) and at 524 nm (ϵ = 8400 M^{-1} cm^{-1}), respectively. Second-order oxidation rate constants were determined by global analysis[34] of all the data using the SPECFIT software (Spectrum Software Associates, Chapel Hill, NC).

Voltammetry and Digital Simulation. Voltammograms were collected using an EG&G Princeton Applied Research 273A poten-

(21) Sistare, M. F.; Holmberg, R.; Thorp, H. H. *J. Phys. Chem. B* **1999**, *103*, 10718−10728.

(22) Rudolph, M.; Reddy, D. P.; Feldberg, S. W. *Anal. Chem.* **1994**, *66*, 595A−600A.

(23) Creutz, C.; Sutin, N. *Proc. Natl. Acad. Sci. U.S.A.* **1975**, *72*, 2858−2862.

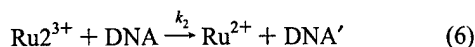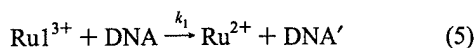(24) Burrows, C. J.; Muller, J. G. *Chem. Rev.* **1998**, *98*, 1109−1151.

(25) Sigma Technical Support, 1997.

(26) Paulson, H. L.; Fischbeck, K. H. *Annu. Rev. Neurosci.* **1996**, *19*, 79−107.

(27) Sutherland, G. R.; Richards, R. I. *Proc. Natl. Acad. Sci. U.S.A.* **1995**, *92*, 3636−3641.

(28) Wells, R. D. *J. Biol. Chem.* **1996**, *271*, 2875−2878.

(29) Chaires, J. B.; Dattagupta, N.; Crothers, D. M. *Biochemistry* **1982**, *21*, 3933−3940.

(30) DeSimone, R. E.; Drago, R. S. *J. Am. Chem. Soc.* **1970**, *92*, 2343−2352.

(31) Welch, T. W.; Corbett, A. H.; Thorp, H. H. *J. Phys. chem.* **1995**, *99*, 11757−11763.

(32) Sambrook, J.; Fritsch, E. F.; Maniatis, T. *Molecular cloning: a laboratory manual*; Cold Spring Harbor: Plainview, NY, 1989.

(33) *CRC Handbook of Biochemistry and Molecular Biology*,3rd ed.; Fasman, G. D., Ed.; CRC Press: Cleveland, OH, 1976; Section B, Vol. 1.

(34) Meader, M.; Zuberbuhler, A. D. *Anal. Chem.* **1990**, *62*, 2220−2224.

tiostat/galvanostat with a single-compartment cell[35] equipped with a tin-doped indium oxide (ITO) working electrode having a geometric area of 0.32 cm² (Delta Technologies), a Pt-wire auxiliary electrode, and a Ag/AgCl reference electrode (Cypress Sytems). ITO electrodes were cleaned as described previously,[36] and a freshly cleaned electrode was used for each experiment. Normal-pulse voltammograms were collected and simulated using the COOL software package according to a published procedure.[31] For cyclic voltammetry experiments, the electrode was conditioned by scanning in buffer between 0.0 and 1.3−1.4 V for seven cycles, followed by a background scan of buffer alone that was subtracted from subsequent scans. Cyclic voltammograms of 50 μM Ru(bpy)$_3^{2+}$ in the absence and the presence of DNA were collected for each electrode. Second-order rate constants for DNA oxidation by Ru(bpy)$_3^{2+}$ were determined by fitting of cyclic voltammetric data using the DigiSim 2.1 software package (Bioanalytical Systems). The complete fitting procedure and parameters used have been described elsewhere.[17,21] Diffusion coefficients of calf thymus and herring testes DNAs were obtained by normal-pulse voltammetry (see below), and those of synthetic oligonucleotides were calculated using the equation of Tirado and Garcia de la Torre.[37−39]

Gel Electrophoresis. Sizes of sheared DNA fragments were determined on a 0.9% agarose gel according to standard procedures.[32] d(GAA)$_n$ and d(AGT)$_n$ (n = 6 or 9) oligonucleotides were 5′-radiolabeled using T4 polynucleotide kinase (New England Biolabs) and 5′-[γ-³²P]dATP (Amersham).[32] Unreacted 5′-[γ-³²P]dATP was removed from the labeled oligonucleotide using a NucTrap column from Stratagene. Radiolabeled oligonucleotide (25−50 000 cpm) was added to a solution of cold oligonucleotide alone (25 μM) or cold oligonucleotide with 30 μM complementary d(TTC)$_9$ or d(ACT)$_9$ oligonucleotide in 50 mM sodium phosphate buffer with 800 mM NaCl. Oligonucleotides were annealed, loaded on a 20% nondenaturing polyacrylamide gel, and electrophoresed at 4 °C and 200 V for 8 h. The gel was exposed on a phosphorimager screen overnight and scanned using a Storm 840 system (Molecular Dynamics).

Results and Discussion

Polymeric DNA: High Salt. (a) Stopped-Flow Spectrophotometry. Our experimental strategy was to study the kinetics of the homogeneous DNA oxidation by stopped-flow spectrophotometry and then to use the results of these experiments in modifying the electrochemical model. Initial investigations centered on reactions at high sodium ion concentration where binding of Ru(bpy)$_3^{3+/2+}$ to DNA can be neglected.[18] As expected from the scan rate dependence of the cyclic voltammetry,[21] single-wavelength kinetic traces exhibited biphasic kinetics and fit best to double-exponential functions (i.e., A_1 exp($-k_1t$) + A_2 exp($-k_2t$)). The ratios of the intensities of the fast and slow components (i.e., A_1:A_2) for these curves were ∼2:1. These ratios were used in subsequent global fitting of the data at multiple wavelengths (350−600 nm), which was performed in SPECFIT according to a kinetic model consisting of two parallel oxidations by noninterconvertible Ru³⁺ populations:

$$\text{Ru}1^{3+} + \text{DNA} \xrightarrow{k_1} \text{Ru}^{2+} + \text{DNA}' \qquad (5)$$

$$\text{Ru}2^{3+} + \text{DNA} \xrightarrow{k_2} \text{Ru}^{2+} + \text{DNA}' \qquad (6)$$

where Ru1³⁺ and Ru2³⁺ indicate species of Ru(III) and the ratio [Ru1³⁺]/[Ru2³⁺] was constrained to a value of 2. A representa-
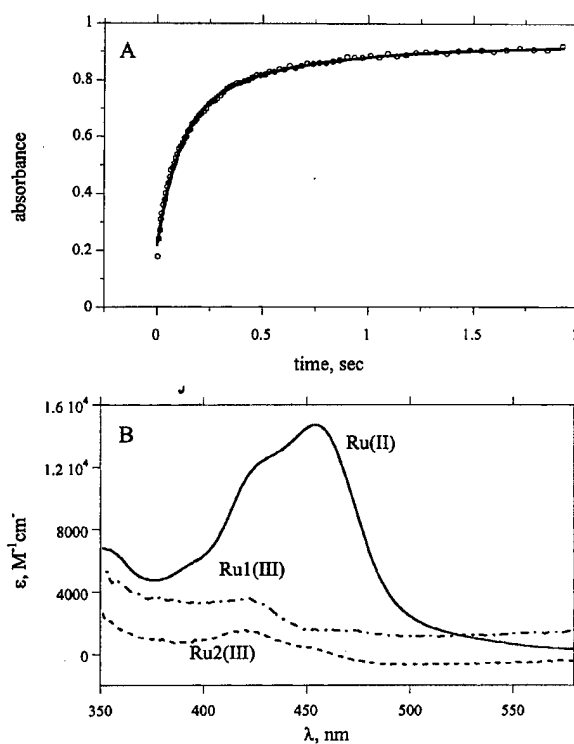
Figure 1. (A) Absorbance at 452 nm versus time for the oxidation of herring testes DNA by Ru(bpy)$_3^{3+}$ at high ionic strength. The solid line shows the calculated time dependence from global analysis. (B) Calculated spectra of Ru²⁺, Ru1³⁺, and Ru2³⁺ determined in the global analysis.

tive kinetic trace at 452 nm with the global analysis fit is shown in Figure 1A. The calculated absorption spectra shown in Figure 1B agree well with the known spectra of Ru(bpy)$_3^{2+}$ and Ru(bpy)$_3^{3+}$.[40] From inspection of the early-time points in Figure 1A, there appears to be another minor contribution from an even faster process not accounted for by the two species in eqs 5 and 6. We have chosen not to analyze this minor process rather than to add another set of parameters, although triexponential processes in DNA have been described.[41,42]

Second-order rate constants in terms of guanine concentration determined by global analysis of the stopped-flow data (as in Figure 1) are summarized in Table 1. A number of important points are apparent. First, the rate constant for the faster component of the reaction of Ru(bpy)$_3^{3+}$ with calf thymus DNA is in excellent agreement with the value we previously reported for this reaction obtained from stopped-flow spectrophotometry with fitting to a single population (24 × 10³ M⁻¹ s⁻¹).[18] Second, the rate constant for the slower component of the reaction of Ru(bpy)$_3^{3+}$ with calf thymus DNA agrees well with the rate constant obtained by chronoamperometry (3.5 × 10³ M⁻¹ s⁻¹).[21] Third, the more abundant Ru1³⁺ population oxidizes guanines in double-stranded DNA almost an order of magnitude faster than Ru2³⁺. This ratio of rates is similar to that obtained for the two observed components in oxidation of calf thymus DNA from recent chronoamperometry experiments at low ionic strength.[21]

(35) Willit, J. L.; Bowden, E. F. *J. Phys. Chem.* **1990,** *94,* 8241−8246.

(36) Welch, T. W.; Thorp, H. H. *J. Phys. Chem.* **1996,** *100,* 13829−13836.

(37) Tirado, M. M.; Garcia de la Torre, J. *J. Chem. Phys.* **1980,** *73,* 1986−1993.

(38) Tirado, M. M.; Garcia de la Torre, J. *J. Chem. Phys.* **1979,** *71,* 2581−2587.

(39) Garcia de la Torre, J.; Lopez Martinez, M. C.; Tirado, M. M. *Biopolymers* **1984,** *23,* 611−615.

(40) Kalyanasundaram, K. *Coord. Chem. Rev.* **1982,** *46,* 159.

(41) Netzel, T. L.; Zhao, M.; Nafisi, K.; Headrick, J.; Sigman, M. S.; Eaton, B. E. *J. Am. Chem. Soc.* **1995,** *117,* 9119−9128.

(42) Netzel, T. L.; Nafisi, K.; Zhoa, M. *J. Phys. Chem.* **1995,** *99,* 17936−17947.

Table 1. Second-Order Rate Constants from Stopped-Flow Spectrophotmetry for Guanine Oxidation by $Ru(bpy)_3^{3+}$

DNA[a]	M	% guanine	[NaCl], mM	k_1,[b] $M^{-1} s^{-1}$	k_2,[b] $M^{-1} s^{-1}$	$\langle k \rangle$, $M^{-1} s^{-1}$
calf thymus	Ru	20	800	$26\,400 \pm 700$	3300 ± 600	$18\,700^c$
	Fe		0	480 ± 40	45 ± 9	260^d
herring testes	Ru	25	800	$34\,100 \pm 800$	5500 ± 300	$24\,600^c$
	Fe		0	720 ± 60	86 ± 4	400^d
$(GAA)_9(TTC)_9$	Ru	16	800	$31\,000 \pm 600$	3900 ± 200	$17\,500^d$
	Fe		0	240 ± 60	26 ± 4	130^d

[a] [G] = [nucleotide phosphate DNA]/5 for calf thymus DNA and nucleotide phosphate DNA/4 for herring testes DNA. [G] = 9 [strand DNA] for the $(GAA)_9(TTC)_9$ oligonucleotide. [b] Each reported value is a mean (± 1 standard deviation) of four to six rate constants at different DNA and metal concentrations. [c] $\langle k \rangle = (2k_1 + k_2)/3$. [d] $\langle k \rangle = (k_1 + k_2)/2$.
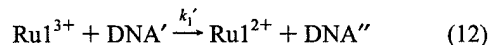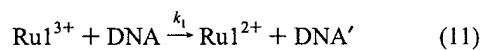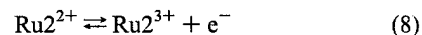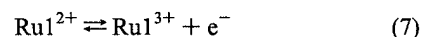
A final point from Table 1 is that both k_1 and k_2 are higher for herring testes DNA than for calf thymus DNA. The rate constants are given in terms of moles of guanine, so the higher fraction of guanine in herring testes DNA is already accounted for in the model. A possible explanation for this increase is a higher number of GG steps in herring testes DNA. The 5′ guanine in GG sequences is more easily oxidized than guanines that are 5′ to other bases due to more favorable stacking interactions with the adjacent guanine.[43-45] As shown previously with defined sequences, larger numbers of GG steps in the sequence increase the apparent rate constant when normalized to the total number of guanines.[45] For comparison, the weighted average rate constants, $\langle k \rangle = (2k_1 + k_2)/3$, are also given in Table 1.

In addition to the two-population model in eqs 5 and 6, two alternative kinetic models were tested. The first involved overoxidation of guanine instead of a parallel oxidation process, since we have shown that overoxidation steps improve the fitting of cyclic voltammetry results and are easily envisioned on the basis of the chemistry of guanine oxidation.[17,21,24] We also examined the possibility of nonproductive Ru^{3+} reduction (i.e., eq 3) accounting for the second exponential in the kinetic trace, since $Ru(bpy)_3^{3+}$ is known to convert independently to the 2+ form at neutral pH.[23] The data were not fit well by either mechanism; these two steps are probably too slow to contribute to the decay on the stopped-flow time scale.

(b) Cyclic Voltammetry. Having established that the homogeneous reaction proceeds with biphasic kinetics and a 2:1 ratio of subpopulations, we next sought to use this information in the electrochemical simulations. However, we first required values for the diffusion coefficients of the biopolymers. These were determined by electrochemistry of a nonoxidizing probe molecule with high DNA-binding affinity, as previously described.[31] Calf thymus DNA and herring testes DNA were sheared to generate shorter and more homogeneous DNA samples. Sizes of these sheared DNA fragments were estimated independently by gel electrophoresis to be between 1000 and 3000 base pairs (bp) for calf thymus (compared to >12 000 bp for unsheared) and between 500 and 1000 bp for herring testes (compared to 700−3000 bp for unsheared). Apparent diffusion coefficients of the fragments were determined using normal-pulse voltammetry with the $Os(bpy)_2(dppz)^{2+}$ intercalator (dppz = dipyridophenazine).[31] This technique provides diffusion coefficients for DNA molecules with an accuracy comparable to that of light-scattering experiments and theoretical calculations.[31,37-39,46,47] Analysis of normal-pulse voltammograms of

$Os(bpy)_2(dppz)^{2+}$ in the presence of sheared calf thymus and herring testes DNAs gave diffusion coefficients of 1.8×10^{-7} and 2.1×10^{-7} cm^2/s, respectively.

With the DNA diffusion coefficients known, the mechanism established by stopped-flow spectrophotometry could then be used as the basis for simulating the electrochemical data. Cyclic voltammograms of $Ru(bpy)_3^{2+}$ in the presence of 1.0, 1.5, and 2.0 mM calf thymus or herring testes DNA at a range of scan rates (10−250 mV/s) were collected. High concentrations and relatively slow scan rates were necessary to observe different amounts of catalytic current enhancement for calf thymus and herring testes DNAs at the same nucleotide concentration. The mechanism employed in the fitting of cyclic voltammograms was similar to the mechanism we have previously reported (eqs 1−4),[17] except that two noninterconvertible ruthenium populations were used for the initial electron transfer, as observed in the stopped-flow studies. The ratio $[Ru1^{3+}]/[Ru2^{3+}] = 2$ was taken from the fitting of the stopped-flow data. Two further oxidations by the more reactive $Ru1^{3+}$ population were required to fit the data, which are in contrast to the stopped-flow spectrophotometry data, where no overoxidation reactions are apparent. The complete mechanism entered into DigiSim simulation program is shown in eqs 7−14, where DNA‴ is DNA that has been oxidized by three electrons.

$$Ru1^{2+} \rightleftharpoons Ru1^{3+} + e^- \qquad (7)$$

$$Ru2^{2+} \rightleftharpoons Ru2^{3+} + e^- \qquad (8)$$

$$Ru1^{3+} \rightleftharpoons Ru1^{2+} \qquad (9)$$

$$Ru2^{3+} \rightleftharpoons Ru2^{2+} \qquad (10)$$

$$Ru1^{3+} + DNA \xrightarrow{k_1} Ru1^{2+} + DNA' \qquad (11)$$

$$Ru1^{3+} + DNA' \xrightarrow{k_1'} Ru1^{2+} + DNA'' \qquad (12)$$

$$Ru1^{3+} + DNA'' \xrightarrow{k_1''} Ru1^{2+} + DNA''' \qquad (13)$$

$$Ru2^{3+} + DNA \xrightarrow{k_2} Ru2^{2+} + DNA' \qquad (14)$$
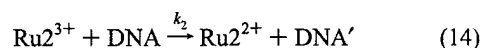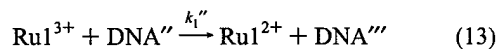
A representative set of cyclic voltammograms overlaid with DigiSim fits is shown in Figure 2A. The rate constants obtained from the simulations did not show a systematic dependence on the DNA concentration and are given in Table 2 as averages from three concentrations at 10 and 250 mV/s for both calf thymus and herring testes DNAs. The values of k_1 agree well with the rate constant we have previously determined for oxidation of guanine in calf thymus DNA at high ionic strength by cyclic voltammetry ($\sim 1 \times 10^4$ $M^{-1}s^{-1}$),[18] where the data were fit to only one population. The ratio of rates for the initial electron transfer in the faster and the slower components varied with the scan rate between 10 and 60, with the lower limit being

(43) Saito, I.; Nakamura, T.; Nakatani, K.; Yoshioka, Y.; Yamaguchi, K.; Sugiyama, H. *J. Am. Chem. Soc.* **1998**, *120*, 12686−12687.
(44) Sugiyama, H.; Saito, I. *J. Am. Chem. Soc.* **1996**, *118*, 7063−7068.
(45) Sistare, M. F.; Codden, S. J.; Heimlich, G.; Thorp, H. H. *J. Am. Chem. Soc.* **2000**, *122*, 4742−4749.
(46) Eimer, W.; Pecora, R. *J. Chem. Phys.* **1991**, *94*, 2324−2329.
(47) Goinga, H. T.; Pecora, R. *Macromolecules* **1991**, *24*, 6128−6138.

Table 2. Second-Order Rate Constants from Electrochemistry for Guanine Oxidation by $Ru(bpy)_3^{3+}$ in Polymeric DNA at High Salt Concentrations

DNA^a	v, mV/s	$10^3 k_1,^b$ M^{-1} s^{-1}	$10^3 k_1',^b$ M^{-1} s^{-1}	$10^3 k_1'',^b$ M^{-1} s^{-1}	$10^3 k_2,^b$ M^{-1} s^{-1}	$\langle k \rangle,^c$ M^{-1} s^{-1}
calf	10	6.2 ± 1.1	5.9 ± 3.0	6.0 ± 3.5	0.59 ± 0.38	4 300
thymus	250	17 ± 3.1	11 ± 1.6	0	0.75 ± 0.30	11 600
herring	10	6.8 ± 1.4	5.1 ± 0.90	5.3 ± 1.4	0.39 ± 0.26	4 700
testes	250	21.4 ± 5.1	12 ± 2.5	0	0.89 ± 0.30	14 600

^{a} [G] = [nucleotide phosphate DNA]/5 for calf thymus and [nucleotide phosphate DNA]/4 for herring testes DNA. ^{b} Each reported value is a mean (± 1 standard deviation) of three rate constants (1.0, 1.5, and 2.0 mM nucleotide phosphate DNA). ^{c} $\langle k \rangle = (2k_1 + k_2)/3$.
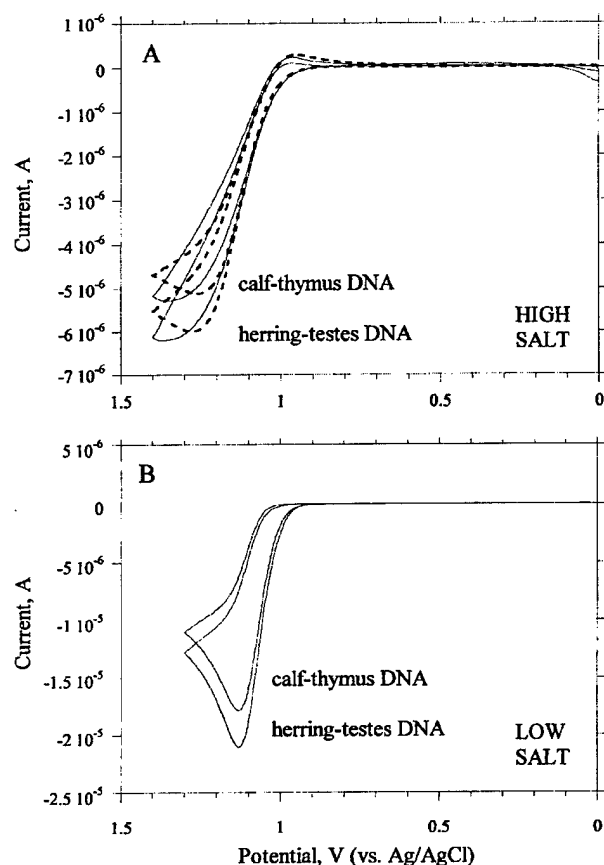
Figure 2. Cyclic voltammograms (solid) and digital simulations (dashed; calculated using eqs 7–14) for 50 μM $Ru(bpy)_3^{2+}$ with 2.0 mM calf thymus or herring testes DNA in (A) 50 mM sodium phosphate, pH 7, with 800 mM NaCl and (B) 50 mM sodium phosphate, pH 7, at 50 mV/s.

in good agreement with the ratio of the two components determined by chronoamperometry.[21]

Rate constants for both the faster and the slower component are lower than those obtained from stopped-flow spectrophotometry. We suspect that this relationship is a result of the longer time scale in the cyclic voltammetric experiment and the subsequent need for the addition of overoxidation steps, which provide an additional pathway for Ru(III) reduction not needed in the stopped-flow model. Accordingly, fitting of cyclic voltammograms collected at higher scan rates, i.e., shorter reaction times, required fewer overoxidation steps and gave k_1 values that approach the values obtained in the stopped-flow experiment (Table 2). However, the relative amount of catalytic current enhancement decreases with increasing scan rate because of the lower number of catalytic cycles at shorter reaction times, which leads to a larger error. At present, we are unsure as to whether the overoxidation steps are required because the longer time scale allows for additional reactions or because the

simulation model is in some way limited. Parallel investigation of oxidation products and reaction kinetics should allow us to clarify this point in the future.

As discussed above, our primary goal was to determine whether the inclusion of multiple rate constants in the fitting of the electrochemical data reduces the dependence of the simulated rate constants on the scan rate observed when only one population is used. In Table 2, the rate constants obtained from the simulation of cyclic voltammograms with two populations of Ru(III) do show a modest scan rate dependence: the values of k_1 and k_1' increase with an increase in scan rate and the value of k_1'' becomes negligible at 250 mV/s. The values of k_2 do not change in a systematic fashion over the studied range of scan rates. Although the rate constants in Table 2 still show an experimentally significant scan rate dependence, the variation is much less pronounced than when only one population is used in the fit. In Table 2, the value of k_1 changes by a factor of 2 from 10 to 250 mV/s, which is much smaller than the scan rate dependence of the rate constant when only one ruthenium population is entered in the mechanism. In the latter case, the apparent rate changes by an order of magnitude on going from 25 to 250 mV/s.[21] Thus, use of two ruthenium populations reduces the scan rate dependence previously observed by digital simulation, supporting the proposal that biphasic kinetics in the guanine–Ru(III) electron transfer are responsible for the scan rate dependence.

Polymeric DNA: Low Salt. (a) Stopped-Flow Spectrophotometry. Studies on calf thymus and herring testes DNA were performed at low ionic strength to examine the effect of ruthenium binding to the DNA on the kinetics of guanine oxidation in the two polymers containing different amounts of guanine. Binding of $Ru(bpy)_3^{3+}$ to DNA in the absence of additional NaCl renders the rate of guanine oxidation approximately an order of magnitude faster than at high ionic strength,[17] making it difficult to study by stopped-flow spectrophotometry. To follow the faster reaction at low ionic strength, we decided to employ $Fe(bpy)_3^{3+}$, which is a close structural analogue of $Ru(bpy)_3^{3+}$ but has a lower redox potential ($E_{1/2}$ [Fe(III/II)] = 0.85 V), slowing the rate of guanine oxidation considerably.[18] The reaction was monitored at 524 nm in the same manner as the reaction of DNA with ruthenium at high ionic strength. SPECFIT analysis was also performed analogously to that for the ruthenium case, using the same mechanism (eq 5 and 6). The ratio of two iron populations was established by fitting of a double exponential to single-wavelength data and gave a ratio of $[Fe1^{3+}]/[Fe2^{3+}] = 1$, which differs from the 2:1 ratio of two ruthenium populations at high ionic strength. The difference in the ratios of the faster and the slower components is probably not significant. Second-order rate constants in terms of guanine concentrations for calf thymus and herring testes DNAs at various DNA concentrations are summarized in Table 1. The ratio of rate constants for the faster and slower component is similar to the ratio of the two components at high ionic strength, but the difference in rates of guanine oxidation in calf

thymus and herring testes DNAs is much more pronounced when binding of the metal complex is occurring, giving nearly a factor of 2 difference between herring testes and calf thymus DNAs. This difference could be due to an even more greatly enhanced reactivity of GG steps at low ionic strength compared to high ionic strength.

(b) Cyclic Voltammetry. Electrochemical studies on polymeric DNA substrates were also performed under conditions where metal complex binding to the polyanion must be considered. Cyclic voltammograms of $Ru(bpy)_3^{2+}$ at low ionic strength in the presence of 1.0, 1.5, and 2.0 mM calf thymus or herring testes DNA at 25 and 50 mV/s were collected; representative data are shown in Figure 2B. While the amount of current is much higher than that in the high ionic strength case, the binding of ruthenium to DNA does not enhance the relative difference in the amount of current enhancement in the presence of different amounts of guanine. This result demonstrates that small differences in the guanine content (20% vs 25%) can be detected in our system regardless of the ionic strength. We were not able to extract rate information from the cyclic voltammograms because the mechanism that accounts for both the ruthenium binding and the presence of the faster and the slower components has too many parameters, which were therefore not well determined.

Oligonucleotides. (a) Stopped-Flow Spectrophotometry— High Salt. Stopped-flow spectrophotometric studies with Ru-$(bpy)_3^{3+}$ at high ionic strength were extended to smaller DNA molecules, namely, synthetic oligonucleotides containing trinucleotide repeat sequences. We chose to investigate the trinucleotide repeat effect in oligonucleotides based on $(GAA)_n$, which is expanded in the genomes of Friederich's ataxia patients.[26-28] This motif was chosen over other physiologically relevant sequences because of the lack of guanines in the complementary strand, which makes possible direct comparison the data for single- and double-stranded oligonucleotide in subsequent voltammetry experiments. The rate constants for oxidation of guanine in the double-stranded $(GAA)_9(TTC)_9$ oligonucleotide were extracted from stopped-flow data in the same manner as that used for the case of polymeric DNA molecules and are shown in Table 1. The most important observation is the biphasic nature of the electron-transfer reaction, with the ratio of two Ru^{3+} populations of 1:1. The biphasic kinetics of the reaction with oligonucleotides as the substrate suggests that polydispersity and sequence heterogeneity of DNA molecules are not the origin of the biphasic kinetics since synthetic oligonucleotides are all of the same length and their hybrids are too short to have unusual secondary structures. Rate constants for guanine oxidation are nearly identical in double-stranded oligonucleotides and in polymeric DNA samples (Table 1), which is reasonable since calf thymus and herring testes DNAs are almost completely double-stranded. The ratio of the faster and the slower component also remains constant regardless of the DNA sample. Thus, potential polydispersity in polymeric DNA samples does not appear to affect the rate of electron transfer.

(b) Cyclic Voltammetry—High Salt. Guanine oxidation in oligonucleotides containing triplet repeats was also investigated by cyclic voltammetry. Two trinucleotide repeat sequences were examined: $(GAA)_n$ and $(AGT)_n$, where $n = 6$ or 9. The $(AGT)_n$ repeat was included to study the effect of the base 3' to the guanine, since the GA step in the $(GAA)_n$ repeat may be more reactive than the GT step in the $(AGT)_n$ repeat due to differential stacking of two purines compared to a purine and a pyrimidine.[43]
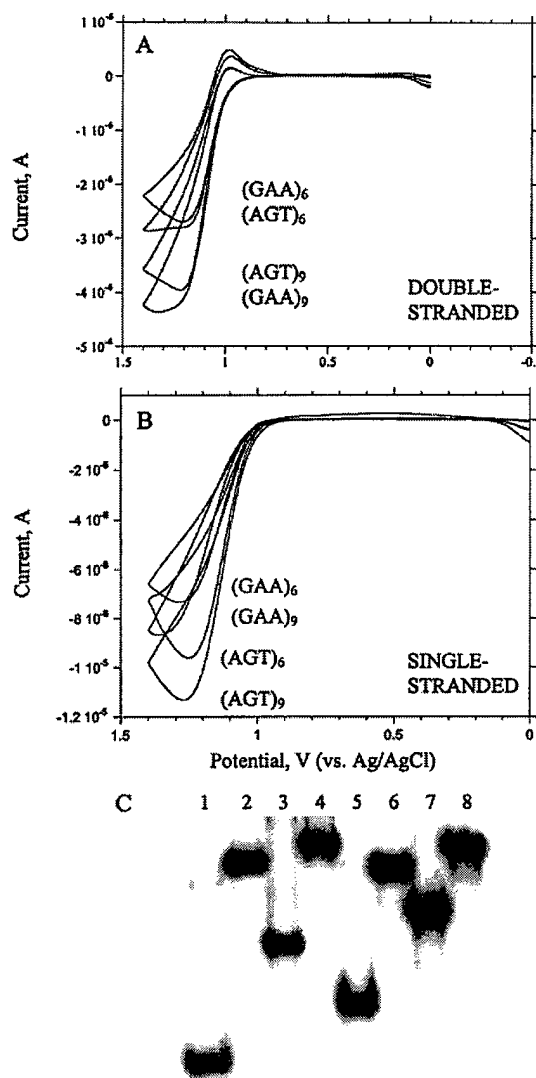
Figure 3. (A, B) Cyclic voltammograms of 50 μM $Ru(bpy)_3^{2+}$ with 25 μM double-stranded (ds) (A) and single-stranded (ss) (B) oligonucleotides in 50 mM sodium phosphate, pH 7, with 800 mM NaCl at 25 mV/s. (C) Nondenaturing polyacrylamide gel of $(GAA)_n$ and $(AGT)_n$ oligonucleotides visualized by phosphorimagery. Lanes: 1, ss $(GAA)_6$; 2, ds $(GAA)_6$; 3, ss $(GAA)_9$; 4, ds $(GAA)_9$; 5, ss $(AGT)_6$; 6, ds $(AGT)_6$; 7, ss $(AGT)_9$; 8, ds $(AGT)_9$.

Representative sets of cyclic voltammograms are shown in Figure 3A,B. Oligonucleotides containing six and nine triplet repeats are easily distinguished when single- or double-stranded. More catalytic current is observed for single-stranded oligonucleotides because of the higher solvent accessibility of single-stranded guanines compared to guanines inside the double helix.[18] Double-stranded $(GAA)_n$ and $(AGT)_n$ oligonucleotides show the same amount of current enhancement within experimental error, whereas single-stranded $(AGT)_n$ oligonucleotides produce more current than $(GAA)_n$ oligonucleotides. We suspected that this difference may be due to the presence of noncanonical secondary structures in $(GAA)_n$ oligonucleotides imposed by the ability of guanine and adenine to form Hoogsteen base pairs.[48] Nondenaturing gel electrophoresis under conditions identical to those in our electrochemical experiments

(48) *Nucleic Acids in Chemistry and Biology*; 2nd ed.; Blackburn, G. M., Gait, M. J., Eds.; Oxford University Press: New York, 1996.
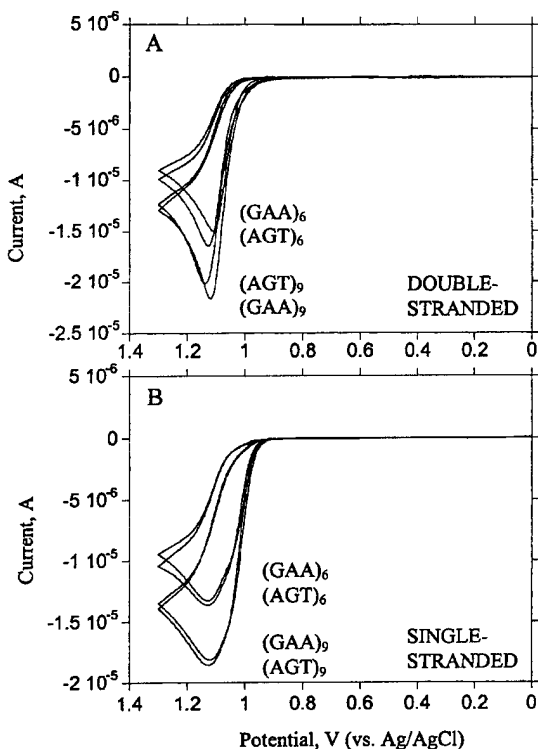
Figure 4. Cyclic voltammograms of 50 μM Ru(bpy)$_3{}^{2+}$ with 25 μM double-stranded (A) and single-stranded (B) oligonucleotides in 50 mM sodium phosphate, pH 7, at 25 mV/s.

(25 μM oligonucleotide in 50 mM sodium phosphate with 800 mM added sodium chloride; Figure 3C) supports this hypothesis, since the single-stranded forms of this oligonucleotide (lanes 1 and 3) migrate much faster than the single-stranded forms of the (AGT)$_n$ sequence (lanes 5 and 7). All of the annealed samples migrate as expected for the duplex forms. The results in Figure 3 provide a satisfying demonstration of how the electrochemistry can indicate changes in structure that can then be confirmed by traditional biochemical techniques.

(c) Cyclic Voltammetry—Low Salt. Cyclic voltammograms of Ru(bpy)$_3{}^{2+}$ in the presence of 25 μM single- and double-stranded (GAA)$_6$, (GAA)$_9$, (AGT)$_6$, and (AGT)$_9$ oligonucleotides at low ionic strength are shown in Figure 4. While the absolute amount of observed current is higher than that observed at high ionic strength (Figure 3), the relative difference between six and nine repeats remains the same both in double- (Figure 4A) and in single-stranded (Figure 4B) oligonucleotides. This situation is analogous to the comparison of calf thymus and herring testes DNAs at low and high ionic strengths and indicates that binding of the metal complex to DNA increases the overall signal but neither improves nor decreases the sensitivity for distinguishing different amounts of guanine. In contrast to the high ionic strength case, single-stranded (GAA)$_n$ and (AGT)$_n$ oligonucleotides show the same amount of current enhancement possibly because the noncanonical secondary structures in (GAA)$_n$ repeats (Figure 3C) form only at high sodium ion concentration.

A striking feature in Figure 4 compared to the voltammograms collected at high ionic strength is the similar currents observed for double- (Figure 4A) and single-stranded (Figure 4B) DNAs. In Figure 3 and in many other experiments performed at high salt concentration, we have observed much higher reactivity of single-stranded and mismatched guanines

due to higher solvent accessibility.[18,49] Tighter binding of the metal cation to the double helix enhances the reactivity of double-stranded oligonucleotides; however, the guanines of single-stranded oligonucleotides are more solvent accessible and therefore more reactive. These effects are apparently contradictory; thus, the difference in absolute current for double- and single-stranded DNAs is small at low salt concentration. The voltammograms do differ in shape, where voltammograms of single-stranded DNA are much wider and voltammograms of double-stranded DNA have much sharper peaks.

(d) Distinguishing Repeat Numbers. In the final set of experiments, we examined the reactivity of oligonucleotides containing (GAA)$_n$ ($n = 5-9$) trinucleotide repeats. Here our goal was to determine whether the catalytic current was sufficient to distinguish addition of a single repeat to the sequence. To combine the advantages of better sensitivity at lower ionic strength and a simpler mechanism at high ionic strength, an intermediate ionic strength regime (50 mM sodium phosphate with 400 mM sodium chloride) was chosen. Cyclic voltammograms of 25 μM single- and double-stranded oligonucleotides at 25 mV/s are shown in Figure 5A,B, and plots of peak current vs number of repeats, n, are shown in Figure 5C. The peak current increases linearly with the number of repeats in both single- and double-stranded (GAA)$_n$ oligonucleotides. More current enhancement is observed in the case of single-stranded oligonucleotides, suggesting that the unbound ruthenium dominates at this ionic strength. However, the amount of current enhancement for (GAA)$_6$ and (GAA)$_9$ oligonucleotides is higher and the difference between single- and double-stranded DNAs is less pronounced when compared to those at high ionic strength (Figure 2), which implies that binding of ruthenium to DNA is detectable.

Conclusions

Biphasic Kinetics. The electron-transfer reaction of M(bpy)$_3{}^{3+}$ (M.= Ru, Fe) with guanine nucleobases exhibits biphasic kinetics both in DNA polymers of heterogeneous sequences and in trinucleotide-repeat oligonucleotides at both high and low ionic strengths. This suggests that conformation, polydispersity, and sequence heterogeneity are not the origin of the two populations. Simple binding of the metal complex is likely not the source of the two populations either, since the two populations are present even when binding of the metal complex is negligible, i.e., at high Na$^+$ concentrations. We believe that the biphasic kinetics result simply from inclusion of guanine in a macromolecule (even in small oligonucleotides), which is supported by many observations of biphasic reaction kinetics for similar reactions.[50−53] As has been discussed elsewhere,[50−53] the two species likely result from different binding geometries that undergo a reaction (in this case electron transfer) that is fast compared to the diffusive interconversion of the two species.

Scan Rate Dependence. The scan rate dependence of the rate constants obtained from cyclic voltammetry is greatly diminished when the voltammograms are fit to the two-population model (Table 2) instead of the mechanism with only

(49) Ropp, P. A.; Thorp, H. H. *Chem. Biol.* **1999**, *6*, 599−605.

(50) Arkin, M. R.; Stemp, E. D. A.; Holmlin, R. E.; Barton, J. K.; Hormann, A.; Olson, E. J. C.; Barbara, P. F. *Science* **1996**, *273*, 475−480.

(51) Arkin, M. R.; Stemp, E. D. A.; Turro, C.; Turro, N. J.; Barton, J. K. *J. Am. Chem. Soc.* **1996**, *118*, 2267−2274.

(52) Barton, J. K.; Kumar, C. V.; Turro, N. J. *J. Am. Chem. Soc.* **1986**, *108*, 6391−6393.

(53) Kumar, C. V.; Barton, J. K.; Turro, N. J. *J. Am. Chem. Soc.* **1985**, *107*, 5518−5523.
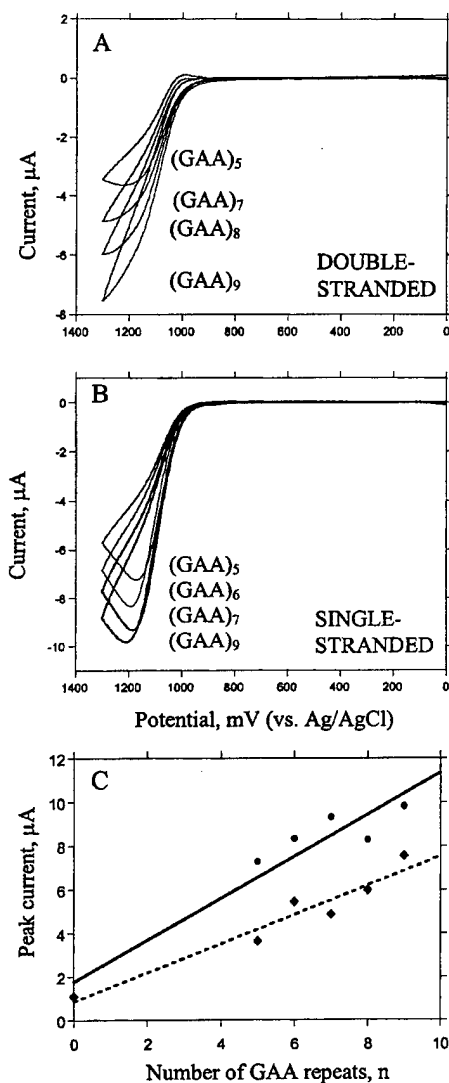
Figure 5. (A, B) Cyclic voltammograms of 50 μM Ru(bpy)$_3{}^{2+}$ with 25 μM double-stranded (A) and single-stranded (B) oligonucleotides in 50 mM sodium phosphate, pH 7, with 400 mM NaCl at 25 mV/s. (C) Plots of peak currents taken from voltammograms for double-stranded (◆) and single-stranded (●) oligonuclotides vs the number of GAA repeats, *n*. Solid and dashed lines are best linear fits of the data; $R = 0.96$.

one population used previously.[17,45] The apparent rate constants obtained from fits to the one-population model are therefore an average of the rate constants for two phases of the reaction with the relative contributions of the two phases varying with the scan rate. Thus, inclusion of the two populations in the model

reduces the effect on the apparent rate constant of sampling a fraction of the reaction course at any given scan rate.

Effect of Guanine Density. Heterogeneous-sequence DNA polymers that differ in their guanine contents by only ~5% are easily distinguished by the current observed in cyclic voltammetry in both high and low ionic strength regimes. This effect is due in part to the increased guanine concentration, which increases the observed current. However, the change in absolute guanine concentration is accounted for in the modeled rate constants, which are given in terms of moles of guanine. Therefore, the polymers with higher guanine content are intrinsically more reactive than those with less. This effect may arise from a higher number of electron-rich GG doublets, which are 12 times more reactive than an isolated guanine.[45] Alternatively, the higher numbers of guanines may provide greater intrinsic reactivity due to an increase in the frequency of collisions that lead to electron-transfer. We have discussed these issues in detail elsewhere and examined these effects in oligonucleotides of known sequences.[21,45] Because the sequences present in calf thymus and herring testes DNAs are heterogeneous, this issue cannot be resolved with certainty.

Guanine-containing trinucleotide repeat sequences of different lengths are readily differentiated at high, low, and intermediate ionic strengths. The observed current enhancement increases linearly with the number of repeats at intermediate ionic strength. This is of special significance because it should allow for future detection of trinucleotide repeat expansion in clinical samples from patients with neurodegenerative disorders such as fragile X syndrome, Friedrich's ataxia, and myotonic dystrophy.[26-28]

Secondary-Structure Dependence. Single-stranded oligonucleotides are much more reactive than their double-stranded counterparts under high ionic strength conditions as a result of higher solvent accessibility of guanine nucleobases. This is not the case in the low-salt regime, where the more pronounced solvent accessibility of single-stranded guanines is counteracted by an enhanced affinity of the positively charged metal complex for the more negatively charged double-stranded DNA, leading to comparable reactivities of single- and double-stranded sequences. Noncanonical secondary structures of (GAA)$_n$ are apparent in the electrochemistry and are verified independently by native gel electrophoresis. These observations demonstrate that detection of guanine secondary structures is best performed at high ionic strength, while simple quantitation of guanine concentrations is best performed at low ionic strength, where different secondary structures exhibit similar rate constants.

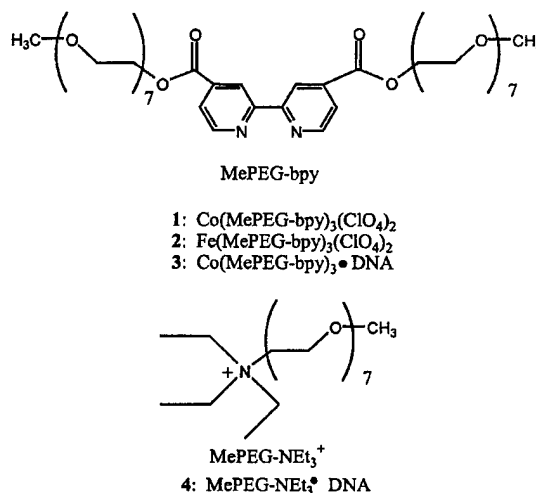# An Ionic Liquid Form of DNA: Redox-Active Molten Salts of Nucleic Acids

Anthony M. Leone, Stephanie C. Weatherly, Mary Elizabeth Williams,†
H. Holden Thorp,* and Royce W. Murray*

Contribution from the Department of Chemistry, Venable and Kenan Laboratories,
University of North Carolina, Chapel Hill, North Carolina 27599-3290

Received September 11, 2000. Revised Manuscript Received November 13, 2000

Abstract: Ionic liquids are described that contain duplex DNA as the anion and polyether-decorated transition metal complexes based on M(MePEG-bpy)$_3^{2+}$ as the cation (M = Fe, Co; MePEG-bpy = 4,4′-(CH$_3$(OCH$_2$-CH$_2$)$_7$OCO)$_2$-2,2′-bipyridine). When the undiluted liquid DNA—or molten salt—is interrogated electrochemically by a microelectrode, the molten salts exhibit cyclic voltammograms due to the physical diffusion (D_{PHYS}) of the polyether−transition metal complex. When M = Co(II), the cyclic voltammogram of the melt shows an oxidative wave due to the Co(III/II) couple at $E_{1/2}$ = 0.40 V (versus Ag/AgCl) and a D_{PHYS} of 6 × 10^{-12} cm^2/s, which is significantly lower than that for Co(MePEG-bpy)$_3$(ClO$_4$)$_2$ (D_{PHYS} = 2.6 × 10^{-10} cm^2/s) due to greater viscosity provoked by the DNA polymer. When a 1:1 mixture is made of the Co(MePEG-bpy)$_3$·DNA and Fe(MePEG-bpy)$_3$(ClO$_4$)$_2$ melts, two redox waves are observed. The first is due to the Co(III/II) couple, and the second is a catalytic wave due to oxidation of guanine in DNA by electrogenerated Fe(III) in the undiluted melt. Independent experiments show that the Fe(III) form of the complex selectively oxidizes guanine in duplex DNA. These DNA molten salts constitute a new class of materials whose properties can be controlled by nucleic acid sequence and that can be interrogated in undiluted form on microelectrode arrays.

The ability of nucleic acids to store and transfer information through Watson−Crick base pairing has intriguing parallels with microelectronic circuitry.[1−3] Binding of complementary DNA sequences has been suggested as a method for forming connections between circuit elements,[3−5] directing assembly of nanoscale structures,[6,7] and computing.[1,8] In addition to providing a molecular self-assembly platform, DNA can also provide specific electronic signals through electron-transfer reactions of the guanine nucleobase.[9−11] Herein, we report on novel ionic liquid materials based on DNA salts of polyether-decorated transition metal complexes (Figure 1) that, in undiluted form, undergo electrochemical reactions and act as catalytic electron relays between a microelectrode and DNA. The DNA remains double-stranded in the ionic liquids, and the electrochemistry is performed under vacuum. The semisolid-state nature of the new DNA materials—which can be regarded as molten salts—may be useful in microelectronic circuits that utilize DNA for

MePEG-bpy

1: Co(MePEG-bpy)$_3$(ClO$_4$)$_2$
2: Fe(MePEG-bpy)$_3$(ClO$_4$)$_2$
3: Co(MePEG-bpy)$_3$•DNA

MePEG-NEt$_3^+$

4: MePEG-NEt$_3^+$ DNA

Figure 1. Structures of the hybrid redox polyether melts. In the melt formed between Co(MePEG-bpy)$_3^{2+}$ and DNA (**3**), there is one Co complex for each base pair of the DNA. In the melt formed with the MePEG-NEt$_3^+$ cation (**4**), there are two ammonium cations per base pair. Elemental analysis of the DNA melts shows that the composition is >90% of the indicated cation−DNA pair with <10% of the perchlorate or chloride salt of the polyether cation. Very little sodium ion was detected in either **3** or **4**, showing that the polyether cation replaced all of the DNA cations during the dialysis.

both self-assembly and electronic connections. Further, the ability to control DNA sequence and secondary structure will allow creation of new classes of molten materials that undergo well-defined structural changes programmed by sequence and monitored by electrochemical signals.

† Present address: Department of Chemistry, Northwestern University, 2145 Sheridan Road, Evanston, Illinois 60208.

(1) Adelman, L. M. *Science* **1994**, *266*, 1021−1024.
(2) Hopfield, J. J.; Onuchic, J. N.; Beratan, D. N. *Science* **1988**, *241*, 817−820.
(3) Mirkin, C. A.; Taton, T. A. *Nature* **2000**, *405*, 626−627.
(4) Porath, D.; Bezryadin, A.; de Vries, S.; Dekker, C. *Nature* **2000**, *403*, 635−639.
(5) Fink, H. W.; Schonenberger, C. *Nature* **1999**, *398*, 407−410.
(6) Mirkin, C. A. *Inorg. Chem.* **2000**, *39*, 2258−2272.
(7) Elghanian, R.; Storhoff, J. J.; Mucic, R. C.; Letsinger, R. L.; Mirkin, C. A. *Science* **1997**, *277*, 1078−1081.
(8) Pirrung, M. C.; Connors, R. V.; Odenbaugh, A. L.; Montague-Smith, M. P.; Walcott, N. G.; Tollett, J. J. *J. Am. Chem. Soc.* **2000**, *122*, 1873−1882.
(9) Hall, D. B.; Holmlin, R. E.; Barton, J. K. *Nature* **1996**, *384*, 731−735.
(10) Johnston, D. H.; Cheng, C.-C.; Campbell, K. J.; Thorp, H. H. *Inorg. Chem.* **1994**, *33*, 6388−6390.
(11) Schuster, G. B. *Acc. Chem. Res.* **2000**, *33*, 253−260.

Redox-Active Molten Salts of Nucleic Acids

J. Am. Chem. Soc., Vol. 123, No. 2, 2001 219
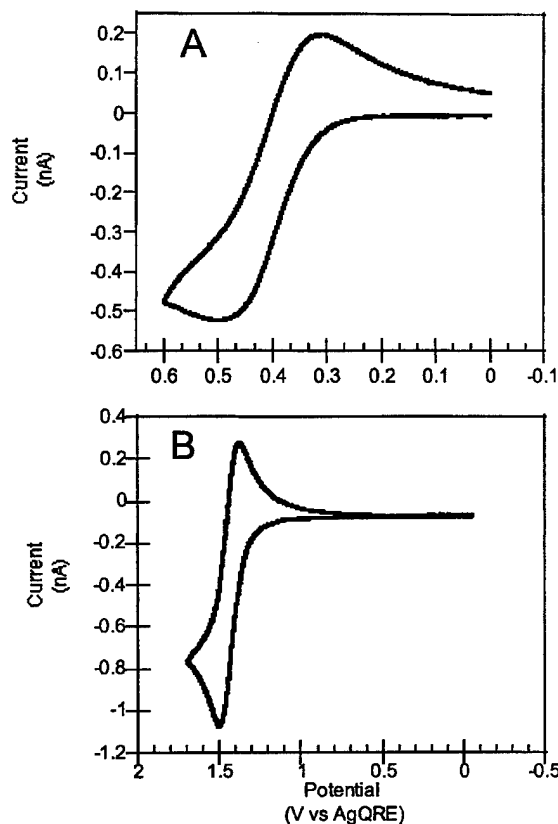
Experimental Section

Materials and Measurements. Compounds **1** and **2** were prepared according to a published procedure[12] and characterized by NMR and electrochemistry. The MePEG-NEt₃Cl salt was prepared according to a published procedure.[13] Electrochemical measurements were conducted under vacuum at 67 °C on 3-electrode arrays with a 3.9 μm radius Pt working electrode as previously described.[12] CD spectra were acquired on an Aviv Model 62DS circular dichroism spectrometer with a 0.1 cm cell. Values of D_{PHYS} were determined from chronoamperometry data plotted as current versus $t^{-1/2}$; and linear fits were used to determine D_{PHYS} as described previously.[12] The bulk concentration of the Co complex was 0.4 M in **3** and 0.2 M in the 1:1 **3/2** melt.

Preparation of DNA Ionic Liquids. Herring testes DNA was obtained from Sigma and sheared to a size range of 50–100 bp as determined by agarose gel electrophoresis. To form compound **3**, 41.0 mL of 49 mM sheared HT DNA (2.0 mmol) was added to 1.0 mmol of **1**. The solution was diluted to 300 mL and added to Millipore brand 500 MWCO dialysis tubing that had been soaked twice for 30 min in Nanopure water. Dialysis was executed for 1 week during which the 8-L reservoir was replaced every 12 h. Following dialysis, the solution was removed from the dialysis tubing, and the water was removed by rotary evaporation at ambient temperature. The resulting melt was rinsed repeatedly with Nanopure water. Removal of water produces a viscous, transparent material that was further dried under vacuum. Elemental analysis gave P = 1.90%, Na = 0.04%, Cl = 0.77%, and Co = 1.90%. Complete conversion to Co(MePEG-bpy)₃·DNA would give P = 1.75%, Na = 0%, Cl = 0%, and Co = 1.66%. Compound **4** was prepared by the same method except that 2 mmol of MePEG-NEt₃Cl was used as was 100 MWCO dialysis tubing. Elemental analysis of **4** gave P = 4.63%, Na = 0.20%, and Cl = 0.87%. Complete conversion to MePEG-NEt₃·DNA would give P = 3.90%, Na = 0%, and Cl = 0%.

Gel Electrophoresis. Compound **2** was oxidized to the Fe(III) form by reaction with 1 equiv of Ce(ClO₄)₄ + 2HClO₄ in an acetonitrile/perchloric acid solution (GFS Chemicals, Powell, OH). Complete oxidation to the Fe(III) form was confirmed by absorbance spectroscopy. In the cleavage reactions, a 10-μL solution of 5′-³²P labeled oligonucleotide (5′-AAAAATATAGTATAAAAAA-3′) and 1 equiv of calf thymus DNA was mixed with 10 μL of either a 1 mM solution of oxidized **2, 2** that had not been oxidized, or Ce(IV) alone. The reaction was allowed to proceed until the Fe(III) was converted to Fe(II) (the color of the solution changed from green to violet). The samples were ethanol precipitated, piperidine treated, and electrophoresed on a denaturing polyacrylamide gel according to a published procedure.[14] A single cleavage site was detected on the gel at the guanine nucleotide upon reaction with oxidized **2** (the site of reaction was determined by comparison with a Maxam–Gilbert G reaction). No cleavage was observed upon reaction with **2** that had not been oxidized or with Ce-(IV) in the absence of **2**.

Results and Discussion

Room temperature melts are reliably formed when one partner in a cation/anion pair is decorated with poly(ethylene glycol) tails of appropriate length (Figure 1)[12,13] and are redox-active molten salts when one of the partners is also capable of electron transfer.[12,13] The polyether tail can be attached to either the redox-active partner or the redox-inert counterion.[13] For example, the perchlorate salt Co(MePEG-bpy)₃(ClO₄)₂ (**1**), containing a redox-active metal complex with polyether tails, is a molten material.[12] When this highly viscous, amorphous compound is placed on a three-electrode array containing a 3.9 μm radius Pt microelectrode, an electrochemical signal due to the Co(III/II) oxidation reaction (0.18 V, all potentials in the text are versus Ag/AgCl) is observed in the neat liquid (Figure 2A).

(12) Williams, M. E.; Masui, H.; Long, J. W.; Malik, J.; Murray, R. W. *J. Am. Chem. Soc.* **1997**, *119*, 1997–2005.

(13) Dickinson, E. V.; Williams, M. E.; Hendrickson, S. M.; Masui, H.; Murray, R. W. *J. Am. Chem. Soc.* **1999**, *121*, 613–616.

(14) Farrer, B. T.; Thorp, H. H. *Inorg. Chem.* **2000**, *39*, 44–49.

Figure 2. Cyclic voltammograms for (A) **1** and (B) **2** at 25 mV/s on the 3.9 μm Pt microelectrode with a silver quasireference and a Pt auxiliary electrode. Measurements were performed at 67 °C under vacuum using a home-built potentiostat capable of detecting 0.1 pA of current. The potentials in the figure are as-collected versus the silver quasireference, but those quoted in the text are versus aqueous Ag/AgCl after conversion with a ferrocene standard.

Diffusion-controlled currents in polyether melts reflect the summed rates of physical diffusion (D_{PHYS}) of the metal complex to the microelectrode and of electron hopping (self-exchange) between oxidized and reduced forms of the complex in the melt,[12] as embodied in the Dahms–Ruff equation:[15]

$$D_{APP} = D_{PHYS} + \frac{k_{EX}\delta^2 C}{6} \qquad (1)$$

where D_{APP} is the overall (apparent) diffusion coefficient, k_{EX} is the rate constant for self-exchange, and C and δ are the concentration and average center-to-center distances between the complexes in the melts, respectively. For the Co(III/II) wave observed in **1**, electron hopping is slow, and the observed current is solely a function of D_{PHYS}. The value of D_{PHYS} for **1** is 2.6 × 10⁻¹⁰ cm²/s; such slow diffusion is typical of the polyether melts.[12] When Co is replaced with Fe to form Fe(MePEG-bpy)₃-(ClO₄)₂ (**2**), the Fe(III/II) oxidation wave appears at 1.04 V and electron hopping is much faster (while D_{PHYS} remains constant), giving higher overall currents (Figure 2B). The larger k_{EX} for Fe compared to Co is a well-understood chemical difference.[12,16] We will show below analogous electrochemical behavior of

(15) Majda, M. In *Molecular Design of Electrode Surfaces*; Murray, R. W., Ed.; John Wiley and Sons: New York, 1992; p 159. Dahms, H. *J. Phys. Chem.* **1968**, *72*, 362. Ruff, I.; Botar, L. *J. Chem. Phys.* **1985**, *83*, 1292.

(16) Buttry, D. A.; Anson, F. C. *J. Am. Chem. Soc.* **1983**, *105*, 685–689.

metal complex molten salts containing DNA and exhibiting evidence of its electron-transfer chemistry.
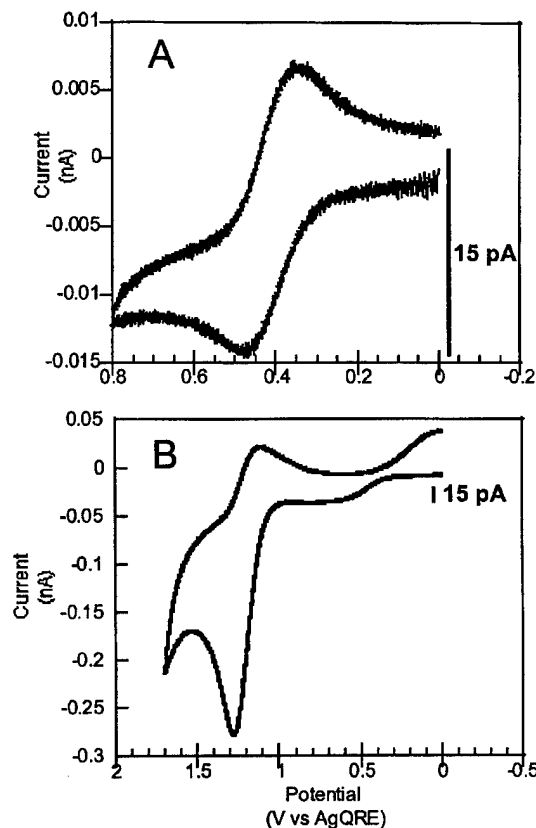
One-electron oxidation of the guanine base has been extensively scrutinized as a partial origin of oxidative DNA damage[17,18] and as a probe of long-range electron transfer along the DNA helix.[9,11,19–22] Transient formation of oxidized guanine bases appears to play a critical role in the ability of DNA to mediate remote electron transfer between two attached circuit elements where those circuit elements can either be molecular donors and acceptors or electrodes.[4,11,22–24] While direct transfer of electrons from guanine to solid electrodes in fluid, homogeneous solutions is slow, guanine oxidation can be studied indirectly by electrochemically generating small molecule redox catalysts.[10,25] Transition metal complexes with potentials ≥ 1.0 V, such as $Ru(bpy)_3^{2+}$ (bpy = 2,2′-bipyridine), mediate guanine electron transfer from intact DNA molecules according to the reaction scheme:[26–28]

$$Ru(bpy)_3^{2+} \rightarrow Ru(bpy)_3^{3+} + e^- \qquad (2)$$

$$Ru(bpy)_3^{3+} + DNA \rightarrow Ru(bpy)_3^{2+} + DNA_{ox} \qquad (3)$$
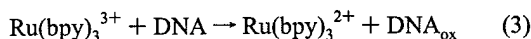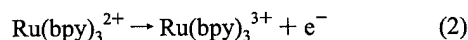
where DNA_{ox} is a DNA molecule with a guanine residue that is oxidized by one electron. Precise potentials are difficult to determine in the melts, so complex **2** was dissolved in ether and determined to have a potential of 1.04 V by use of an internal ferrocene standard. Thus, complex **2** should be capable of oxidizing guanine in DNA in reactions analogous to eqs 2 and 3.

A DNA melt was prepared by equilibrium dialysis of a solution of **1** and herring testes DNA at a stoichiometry of two nucleotides of DNA per one dicationic Co complex. After extensive dialysis to remove the perchlorate counterions from **1** and the sodium cations from DNA, the solution was placed on a rotary evaporator to yield a highly viscous melt, Co-(MePEG-bpy)₃·DNA (**3**). Compound **3** was dried under vacuum, and elemental analysis showed a purity of $\geq 90\%$ with virtually no detectable sodium ion present, indicating that all of the DNA counterions had been replaced by $Co(MePEG\text{-}bpy)_3^{2+}$. The remainder of the composition of **3** is made up of some perchlorate anions in place of DNA.

The cyclic voltammogram of **3** showed a characteristic oxidation wave for the Co(III/II) couple at $E_{1/2} = 0.40$ V (Figure 3A) with currents considerably lower than those for the perchlorate melt **1**. Chronoamperometry experiments were performed, and the collected current was plotted as a function

(17) Henle, E. S.; Linn, S. *J. Biol. Chem.* **1997**, *272*, 19095–19098.

(18) Beckman, K. B.; Ames, B. N. *J. Biol. Chem.* **1997**, *272*, 19633–19636.

(19) Saito, I.; Takayama, M.; Sugiyama, H.; Nakatani, K.; Tsuchida, A.; Yamamoto, M. *J. Am. Chem. Soc.* **1995**, *117*, 6406–6405.

(20) Meggers, E.; Michel-Beyerle, M. E.; Giese, B. *J. Am. Chem. Soc.* **1998**, *120*, 12950–12955.

(21) Lewis, F. D.; Wu, T.; Zhang, Y.; Letsinger, R. L.; Greenfield, S. R.; Wasielewski, M. R. *Science* **1997**, *277*, 673–676.

(22) Wan, C.; Fiebig, T.; Kelley, S. O.; Treadway, C. R.; Barton, J. K.; Zewail, A. H. *Proc. Natl. Acad. Sci. U.S.A.* **1999**, *96*, 6014–6019.

(23) Jortner, J.; Bixon, M.; Langenbacher, T.; Michel-Beyerle, M. E. *Proc. Natl. Acad. Sci. U.S.A.* **1998**, *95*, 12759–12765.

(24) Lewis, F. D.; Liu, X.; Liu, J.; Miller, S. E.; Hayes, R. T.; Wasielewski, M. R. *Nature* **2000**, *406*, 51–53.

(25) Johnston, D. H.; Glasgow, K. C.; Thorp, H. H. *J. Am. Chem. Soc.* **1995**, *117*, 8933–8938.

(26) Johnston, D. H.; Thorp, H. H. *J. Phys. Chem.* **1996**, *100*, 13837–13843.

(27) Sistare, M. F.; Holmberg, R. C.; Thorp, H. H. *J. Phys. Chem. B* **1999**, *103*, 10718–10728.

(28) Szalai, V. A.; Thorp, H. H. *J. Phys. Chem. B* **2000**, *104*, 6851–6859.

Figure 3. Cyclic voltammograms of (A) **3** and (B) a 1:1 mixture of **2** and **3**. Conditions were the same as in Figure 2.

of $t^{-1/2}$. These plots were linear, and the slope was used along with the Cottrell equation as described previously[12] to give a D_{PHYS} for the complex in the DNA melt of 6×10^{-12} cm²/s. The peak current in cyclic voltammograms was also a linear function of the square root of the scan rate and gave a D_{PHYS} of 5×10^{-12} cm²/s. A smaller D_{PHYS} in the DNA melt (compared to the perchlorate melt) is not surprising, since the polymeric counterion provokes a qualitatively higher viscosity and the relatively rigid helices should impede transport of the metal complex to the electrode.

The DNA in the melts is double-stranded. Compound **3** was dissolved in water, and the DNA fragments were separated on an agarose gel. The DNA fragments on the gel were 50–100 bp in length and stained well with ethidium bromide. Since heterogeneous polynucleotides such as herring testes DNA cannot reanneal, this experiment shows that the DNA in the melt was double-stranded. To confirm this point, another melt was prepared using a polyether-decorated ammonium cation, which formed a 1:1 melt with DNA nucleotides, MePEG-NEt₃· DNA (Figure 1, **4**). Compound **4** was characterized by elemental analysis and NMR and was found to give a CD spectrum in water that was identical with that for native herring testes DNA (Figure 4). Compound **3** could not be characterized by CD spectroscopy because the absorptions for the metal complex interfered with the DNA signals. This experiment further demonstrates that the DNA molecules in the melt remain double-stranded. Because **4** contains a countercation that does not exhibit optical absorption in the 250–300 nm range, the melt could be placed between glass plates and scanned in an optical spectrometer. The absorbance spectrum of the neat DNA melt is similar to that of DNA in solution. A pictorial representation

Redox-Active Molten Salts of Nucleic Acids

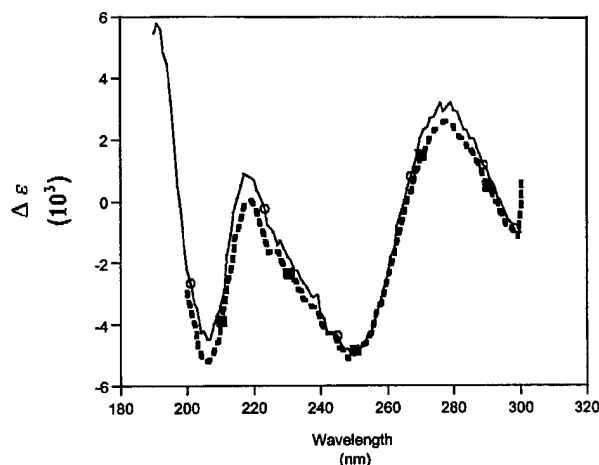*J. Am. Chem. Soc., Vol. 123, No. 2, 2001* 221

Figure 4. CD spectra of 500 μM herring testes DNA (dashed) and **4** (solid). Concentrations are in nucleotide phosphate.

of **3** showing the relative sizes of the polyether tails and DNA is shown in Figure 5.

The only electrochemical signal seen in melt **3** is that due to the Co(III/II) couple. Co(III) is not a sufficiently powerful oxidant to oxidize guanine. However, when a 1:1 mixture was made of **3** and the iron perchlorate melt **2**, two electrochemical signals were observed (Figure 3B). The first was due to the Co(III/II) wave, while the more positive wave for Fe(III/II) displayed an oxidation current much larger than the subsequent reductive current, which is characteristic of mediated electrocatalysis.[29] Faster potential scanning gave a more symmetrical Fe(III/II) wave, and repeated scanning led to smaller oxidation currents on successive scans; both of these features are indicative of electrocatalytic oxidation of guanine.[26,30,31] This behavior is ascribed to catalytic oxidation of guanine in DNA by the electrogenerated Fe(III) in the melt. The Co(III/II) couple was used in choronoamperometry experiments to determine a value of D_{PHYS} for the 1:1 **3/2** melt of 6×10^{-11} cm^2/s, which is higher than in compound **3** probably because of the higher ethylene oxide/DNA ratio.

To verify that guanines were the source of the electrons that gave the catalytic current in Figure 3B, we performed an experiment in which the tailed Fe(III) complex was reacted with a radiolabeled oligonucleotide containing a single guanine. This reaction was performed by oxidizing the Fe(II) complex with Ce^{4+} and mixing the resulting Fe(III) form with DNA in dilute aqueous solution. The DNA showed selective cleavage at the guanine residue following piperidine treatment and high-resolution gel electrophoresis. In addition, cyclic voltammetry of both **3** and **4** in the absence of Fe showed no faradaic current at potentials up to 1.5 V, showing that direct oxidation of guanine at the microelectrode does not occur at a detectable rate. We therefore ascribe the catalytic current observed in Figure 3B to oxidation of guanine by Fe(III) *in the neat DNA molten salt.*

Conclusions

The use of polyether-tailed cations to prepare ionic liquid forms of DNA raises many exciting possibilities. Tailed quaternary ammonium salts of DNA have been used to prepare
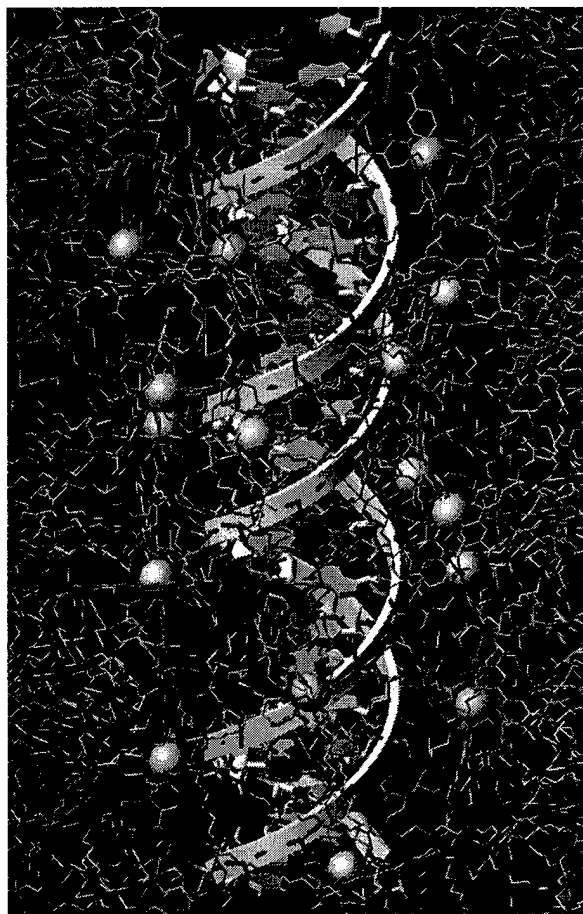

Figure 5. Model showing the structure of **3** with the tailed metal complexes and the DNA molecule rendered to scale. The DNA is shown in a cartoon form and the metal complexes are shown with the metal atoms as blue spheres and the MePEG ligands in CPK colors. The polyether chains provide considerable "solvent" for the DNA molecule and diffusion of the metal ions to the electrode. Note that, for clarity, the drawing shows fewer than the actual 1 metal ion per base pair present in the melt. The model was generated using the Cerius2 software package from MSI.

aligned DNA films,[32] but these materials are not expected to possess favorable electrochemical characteristics because the tail contains only four polyether units with a C$_{10}$ aliphatic unit on the end. The DNA materials **3** and **4** have long polyether tails terminated with only a methyl group, which facilitates ion transport and an ability to interrogate the neat liquid **3** electrochemically. Since the rate of electron hopping for Co-(III/II) is slow, the currents in Figure 3 can be confidently assigned as arising from slow, physical diffusion of the Co complex in the melt. These experiments are carried out on dried materials under vacuum. The melts also show solubility in a wide range of fluid solvents, and both the dissolved forms and the neat melts are amenable to spectroscopic analysis. Recovery of the DNA from the melts and subsequent analysis shows that it is double-stranded. This new ionic phase of DNA is readily manipulated, and the cast films can be deposited onto microelectrode arrays, placed under vacuum, and still exhibit chemical reactions normally observed in dilute solution.

In these melts doped with the Fe complex, the polyether—metal complex serves a dual role: to provide a "solvent" in

(29) Bard, A. J.; Faulkner, L. R. *Electrochemical Methods*; John Wiley and Sons: New York, 1980; p 431.

(30) Szalai, V. A.; Thorp, H. H. *J. Am. Chem. Soc.* **2000**, *122*, 4524–4525.

(31) Armistead, P. M.; Thorp, H. H. *Anal. Chem.* **2000**, *72*, 3764–3770.

(32) Okahata, Y.; Kobayashi, T.; Tanaka, K.; Shimomura, M. *J. Am. Chem. Soc.* **1998**, *120*, 6165–6166.

which diffusive electron transfers can occur and to mediate electron transfer from guanine to the electrode. Numerous pathways for electron transfer exist in the melts, because electrons can transfer from the guanine to the metal, from guanine to an oxidized guanine, and from metal to metal. Guanine—guanine electron transfers may occur within single DNA molecules; however, because of the relatively high concentration of Fe in the melt and its ability to carry charge by electron hopping in the polyether medium, efficient electron transfer within DNA is probably not required. In the future, we believe that these processible ionic liquid materials will provide a simple basis for microstructures that utilize DNA as both a self-assembly partner and, when electron-transfer active poly-ethers such as **3** are used, specific electronic signals. In addition, sequence control of the DNA combined with the maintenance of the duplex structure in the melts provides pathways to new materials where the nucleic acid structure produces designed properties of the polymer melts. The electron-transfer reactivity provides a means to study these properties on small quantities of undiluted material.